The Probing Matter at High Magnetic Fields
with X-Rays and Neutrons Workshop
May 10, 2005
National High Magnetic Field Laboratory

Report from Probing Matter at High Magnetic Fields with X-Rays and Neutrons

Neutron specific contributions compiled by: Garrett Granroth, Collin Broholm, and Frank Klose
X-ray specific contributions compiled by: George Srajer, Zahirl Islam, Young Lee, and Jonathan Lang

October 28, 2005

1 Introduction

The workshop Probing Matter at High Magnetic Fields with X-Rays and Neutrons gathered scientists interested in using High magnetic fields for their research with Neutrons and X-Rays. Many areas of science were discussed. One prominent area of discussion was condensed matter. In these systems magnetic field is a parameter that can be used to induce novel phases of matter. It is a unique parameter because it enters directly into the Hamiltonian as it couples to spin and orbital degrees of freedom. Traditionally, diffraction studies of condensed matter in an applied magnetic field are carried out using neutron scattering. Neutron scattering plays a key role in our understanding of field-dependent phenomena because it is sensitive to the magnetic moments, and also is suitable for studies of magnetic excitations. In recent years research has shown that low-temperature quantum phenomena are very susceptible to impurities and defects. In order to isolate intrinsic properties high-quality and high-purity single-crystal samples are essential which in general come in small (~1mm) sizes. Current state of the art neutron instruments are not able to measure these samples. However with new generation of instruments to be turned on at the SNS these size samples can be studied and third generation high-brilliance x-ray sources are perfectly suited to study such effects on samples this small and smaller. Furthermore x-rays from these new sources can study, subtle symmetry-lowering structural changes occurring locally as well as globally can have profound effects on the underlying physics. Even non-resonant magnetic scattering can easily be used in order to study magnetic long-range order in cuprates, and the resonant magnetic signals from 5d, 4f, and 5f elements are truly enormous.

Each scattering probe has its unique advantages. For x-rays some of these advantages are: elemental selectivity – magnetic signals from different elements can be easily distinguished; very high resolution in q-space; possibility to study valence electron density; possibility to study charge and orbital order using resonant scattering; possibility to separate spin and orbital magnetism. For neutrons some of these advantages are: only sensitive to magnetic interactions with electron cloud; energy scale well matched to the energy scale of magnetic excitations in most systems; elemental sensitivity to hydrogen enabling probes of biological samples; deeply penetrating insensitive, to surface effects. These two short lists illustrate that both techniques are needed to fully illuminate the science described in the following sections in this document. In other words, the ability to examine samples in high magnetic fields at both neutron and X-ray sources is critical.

The report is broken into 4 fundamental areas Section 2 covers the multiple investigations in atomic scale magnetism, Section 3 will discuss manufactured magnetic structures like magnetic thin films and superlattices, Section 4 looks at the study of processing materials in high magnetic fields to provide enhanced engineering properties such as increased strength, and Section 5 will address other topics that were discussed, but not detailed at the meeting. Section 6 summarizes the facility requirements in order to perform the science described in earlier sections. In sections 2-5 we summarize some problems from a broad base of science that were highlighted at this workshop and ideas that were sparked

from discussion at the workshop that will benefit from neutron and x-ray scattering studies.

2 Atomic Scale Magnetism

A central challenge of condensed matter physics is to understand, predict, and control the intricate effects of correlations in many body systems. The correlations can be between any of the constituents of a condensed matter system. High magnetic fields play an important role in the study of two types of correlations that are crucial to understanding many condensed matter systems. These two types of studies are described in separate sections of this document. Section 2.1 describes systems where the correlations are between atomic spins in the system. In these systems there are no conduction electrons to produce additional complicating correlations. Section 2.2 describes systems where correlations between conduction electrons and between conduction electrons and atomic moments are important. This second broad class of materials has scientifically rich field dependent phases waiting to be fully understood by scattering probes.

2.1 Magnetic insulators

From the nano-scale to the macroscopic scale, the properties of insulating magnetic materials are determined by such correlations, and because it is possible to establish accurate microscopic models of these materials, they are ideal laboratories for progress in our basic understanding of condensed matter. Past experimental and theoretical work on insulating magnets was instrumental in developing such important concepts as quasi-particles, critical phenomena, the renormalization group, non-ergodic states of matter, and percolation.

For insulating magnets the energy scale and therefore the field scale required to affect magnetism at the microscopic scale is defined by the magnetic exchange constants of interesting materials[1]. The corresponding field scale varies from fractions of a Tesla to hundreds of Tesla. The importance of access to high magnetic fields is the expansion that this entails in the classes of materials that can be explored in the high field regime defined as $h_{eff} = g\mu_B H / J \approx 1$. Fields up to 10 Tesla allow informative experiments on selected organo-metallic quantum magnets. Fields above 30 Tesla are sufficient to fully magnetize a wide range of such materials, which enables unambiguous determination of the spin Hamiltonian through neutron scattering. 30-40 Tesla is also sufficient to profoundly modify the ground state of a wide range of transition metal oxide quantum magnets.

2.1.1 Quantum Magnetism at High Magnetic Fields

Today there are important new challenges associated with understanding the combined effects of quantum mechanics and strong correlations. How are macroscopic degeneracies resolved through the effects of quantum fluctuations, what are the universal static and dynamical aspects of quantum phase transitions in real materials, and how can the qualitatively different phases that are possible in zero, one, two, and three

dimensional spin systems be classified. The availability of tuning parameters other than temperature, are essential for exploring such questions. An applied magnetic field is a particularly elegant tuning parameter because it is disorder free and couples in a well defined fashion to insulating quantum magnets.

In this section of the report we shall discuss important experiments that a >30 T magnet for neutron scattering would enable in one dimensional, two dimensional, and frustrated quantum magnets. In each case we describe the current scientific challenges and how these could be addressed through neutron scattering experiments in high magnetic fields.

2.1.1.1 Zero Dimensional Magnetism – Molecular Magnets

Interested Participant: Bella Lake
Other interested researchers: David Vaknin, Vasile Garlea, Jerel Zarestky, Marshall. Luban(Ames Laboratory), Stephen Nagler, Andrey Zheludev(Oak Ridge National Laboratory).

Molecular magnetism is a new and exciting area of condensed matter research. Molecular magnets are magnetic objects on the nanoscale that consist of highly symmetric clusters of magnetic ions which interact with each other. Current nanomagnets contain between 2 and 30 transition metal magnetic ions and come in a variety of shapes The original molecular magnets were the ferric wheels where the iron ions formed rings and interacted magnetically with nearest neighbors. These where synthesized in the 1990s and the eight iron wheel $[CsFe_8\{N(CH_2CH_2O)_3\}_8]^+$ or $\{CsFe_8\}$ is shown below. More complex wheel-type structures are now available e.g. the hexadecameric and tetradecameric clusters. Other examples include the cubane-type magnetic molecule $[Cr_8O_4(C_6H_5COO)_{16}]4CH_3CN = \{Cr_8\}$ where the 8 Cr^{3+} ions can be mapped onto the vertices of a cube and interact with each other via two ferromagnetic and two antiferromagnetic exchange constants creating a highly frustrated and entangled system. While $[Mo_{72}Fe_{30}O_{252}(Mo_2O_7(H_2O))_2(Mo_2O_8H_2(H_2O))(CH_3COO)_{12}(H_2O)_{91}].150H_2O = \{Mo_{72}Fe_{30}\}$, consists of 30 spin-5/2 Fe^{3+} ions located at the vertices of an icosidodecahedron and which interact via a single antiferromagnetic exchange constant in a highly frustrated arrangement. Other more complex shapes are also available[2].
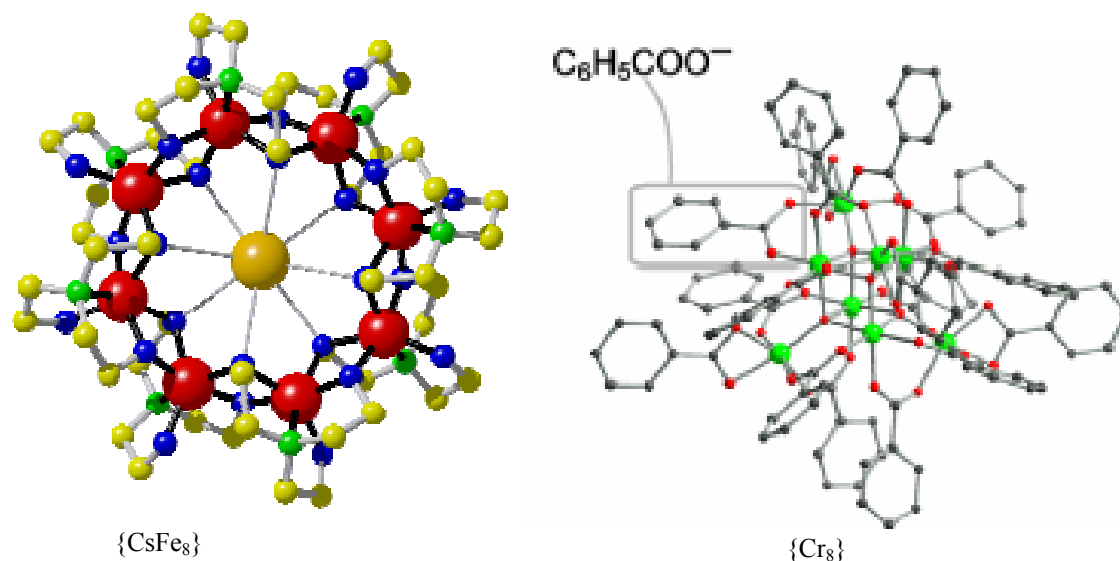
Figure 1 representations of two molecular magnets

The interest in molecular magnets stems among other things from the fact that they can be used to develop and explore concepts of quantum magnetism in the simpler environment of zero-dimensions and with a small number of interacting spins compared to higher dimensional objects with infinite interacting spins normally investigated in condensed matter physics. Despite their apparent simplicity the Hilbert space of these systems is in many cases still too large for exact solutions of the energy levels, hence approximations are required to develop theories and these theories can be readily tested using neutron scattering experiments. Understanding the relevant approximations is highly important and can point the way to theories of much more complex objects. This area of research brings together a number of different disciplines. Using detailed knowledge of organo-metallic chemistry molecular magnets can be tailor-made to investigate a particular physical problem e.g. entanglement, emergent ground states and frustration, by manipulating the physical properties of the molecule e.g. size of magnetic moments, type of magnetic interactions and symmetries. Theories need to be developed, by theoretical physicists or mathematicians and these can then be tested by direct comparison to neutron scattering experiments. Not all energy levels are available to neutron scattering; transitions must involve a change in angular momentum of the system of one unit. However, the ground state of the system can be varied by tuning magnetic field - a technique which allows many more energy levels to be measured. Applied magnetic field therefore plays a crucial role in the exploration of molecular magnets.
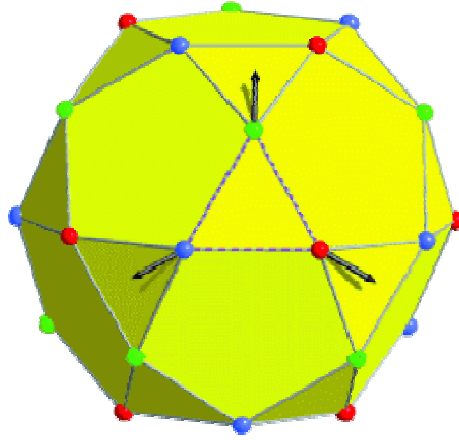
Figure 2 $\{Mo_{72}Fe_{30}\}$ showing only the icosidodecahedral structure of the Fe^{3+} ions. In a classical treatment at low temperatures all of the 30 spins can point in only one of three directions (red, green and blue) and the relative angle between any two nearest neighbor spin directions is 120° (frustrated ordering).

As an example $\{Mo_{72}Fe_{30}\}$ has recently been measured using neutron scattering in both zero field and for fields up to 7T. This molecule consists of triangular arrangements of Fe^{3+} ions and can be used to explore ideas of magnetic frustration and entanglement. An approximate quantum Hamiltonian can be exactly solved[3] and shows good agreement with zero-field neutron scattering measurements over a range of temperatures[4]. Comparison of the in-field data with theory however reveals major differences implying a possible breakdown of the model. Susceptibility measurements show that a field of 18T completely saturates the molecule, i.e., forces all the magnetic moments to point along the field direction and the available fields of up to 7T were inadequate for a complete exploration of the phase diagram. Indeed often a simpler approach for theory is to calculate the excitations in the saturated state and as field is lowered from this value. Considerations of other known molecular magnets show that saturation field can be as high as 100T (e.g. for $\{Cr_8\}$ B_{sat}=27T and for $\{V_6\}$ B_{sat}~100T).
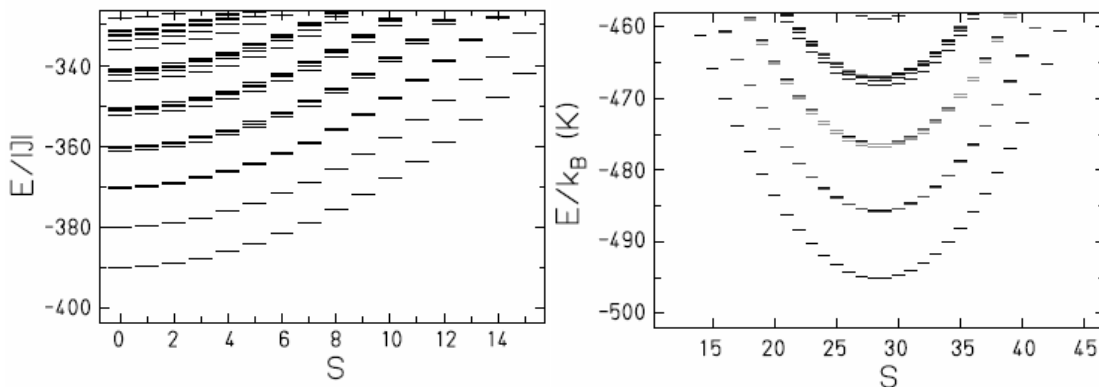
Figure 3 Theoretical energy levels of $\{Mo_{72}Fe_{30}\}$ as a function of total spin and energy. The diagram on the left gives the levels in zero field while the diagram on the right gives the levels for a field of 7T.

2.1.1.2 One Dimensional Magnetism

Interested Participants: Collin Broholm, Mechtilde Enderle, Garrett Granroth, Bella Lake, Mark Lumsden, Igor Zaliznyak
Others Interested Researchers: Martin Greven (Stanford University), Christopher Wiebe(Florida State University), Stephen Nagler, Andrey Zheludev(Oak Ridge National Laboratory)

One dimension is below the critical dimension for long range magnetic order in Heisenberg magnets. While real materials may eventually order due to sub-leading interactions there is generally a temperature regime where quasi-one-dimensional materials are dominated by strong correlations and quantum effects. This makes them particularly important for exploring some of the issues mentioned above. In addition, the simple geometry and low connectivity of one dimensional systems enable a range of powerful theoretical techniques[5].

There are two radically different forms of magnetism in one dimensional spin systems and these are exemplified by the spin-1/2 and the spin-1 uniform Heisenberg antiferromagnetic spin chains. The spin-1/2 antiferromagnetic chain is quantum critical with a gapless magnetic excitation spectrum. The fundamental quasi-particles are extended and strongly interacting topological spin-1/2 objects called spinons that form a Luttinger liquid at T=0. The neutron scattering spectrum takes the form of a gapless bounded continuum (see Figure 4a). This is consistent with spinon quasiparticles as these cannot be individually created or annihilated by the spin-1/2 neutron, rather neutrons scatter through a two-spinon process which implies a bounded continuum at each wave vector[6,7].
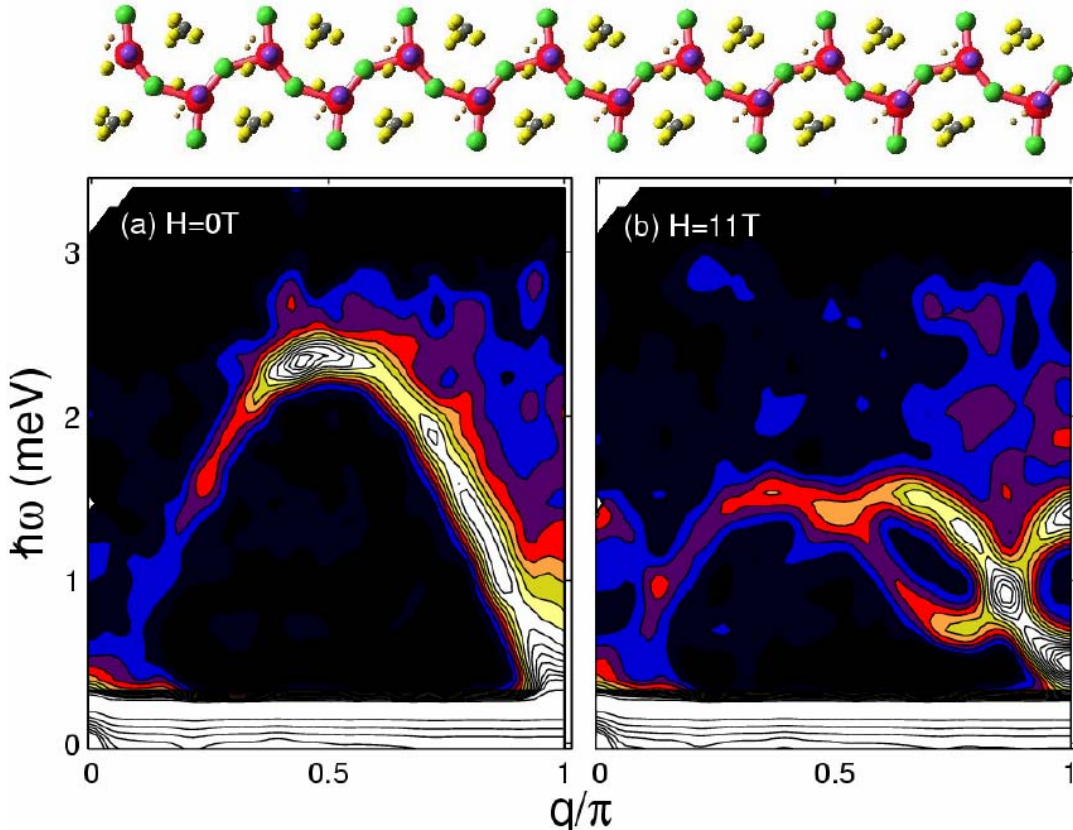
**Figure 4 False color image of neutron scattering from CuCl$_2$ • 2(dimethylsulfoxide) (CDC) (a) in zero field and (b) in a field of 11 Tesla. Spin-1/2 copper atoms, shown in red form spin chains where the lack of bond inversion symmetry leads to an effective staggered field when the system is subjected to a uniform field. The staggered field causes formation of soliton and breathers from spinons as evidenced by resolution limited modes with a finite energy gap. Data from the Disc Chopper Spectrometer at the NCNR and reproduced from (ref. 6).**

High field experiments have already provided important verification of this description in that the soft points of the continua were found shifted to incommensurate wave vectors, which is evidence for a field dependent chemical potential for spinons. In addition as shown in Figure 4b, when there is no center of inversion between spin sites the applied field induces an effective staggered field, which induces spinon binding and a complete alteration in the nature of the magnetic excitations. While theory was in place to describe the effects of a staggered field, the high field experiments[6,8] were the catalyst to developing a full understanding of the profound effects of a staggered field on the quantum critical spin-1/2 chain[9].

The spin-1 chain on the other hand has an energy gap in the excitation spectrum. In a triumph of theoretical physics this gap, which now bears his name, was predicted by F. D. M. Haldane[10] amid strong skepticism throughout the scientific community. The ground state is an isolated singlet that can be described as a state in which each of the two spin-1/2 degrees of freedom that make up a spin-1 site are engaged in singlet formation with one of the spin-1/2 degrees of freedom on the neighboring two sites[11]. Neutron scattering data show a sharp resonant mode in the spectrum that appears to merge with a two particle continuum beyond a momentum threshold[12,13]. Field experiments on spin-1

chains have tracked the splitting of the triplet gap mode, which is complicated by single ion anisotropy effects[14]. Experiments have also explored field induced ordered phases of spin-1 chains[15]. An interesting effect in the spin-1 chain and other gapped spin systems is that impurities can liberate spin degrees of freedom from the otherwise non-magnetic singlet state[16]. While important details vary, other spin chains with an energy gap, such as the spin ladder and the alternating spin chain, have closely related properties. A recent example of such a spin system is $Pb_3V_2O_9$, which has s = 1/2 spins with alternating exchanges in isolated one-dimensional chains[17]. As a result, the material does not order in zero field. However, in applied fields, there is an induced magnetic ordering. The magnitude of these ordered moments is ~0.2μ_B. It was demonstrated that with the high-resolution polarization analysis setup one can study the 3D ordered AF structure in the AFI YBCO compound very close to the Neel temperature where the ordered moment is ~0.1 μ_B using non-resonant magnetic x-ray scattering experiment. Such a setup is also suitable for studying subtle structural distortions that may lower the symmetry of the lattice in field, which would have profound effects on the physics of such materials. An analysis of the power-law boundary between the paramagnetic and ordered states implies that there could be a Bose-Einstein Condensation of magnetic excitations (triplons), but this can only be confirmed with neutron scattering. As well, the evolution of the ordering, which reaches a saturation at ~ 36.8 T, has not been investigated with scattering techniques. Both of these are well-suited to neutron work with this new beamline.
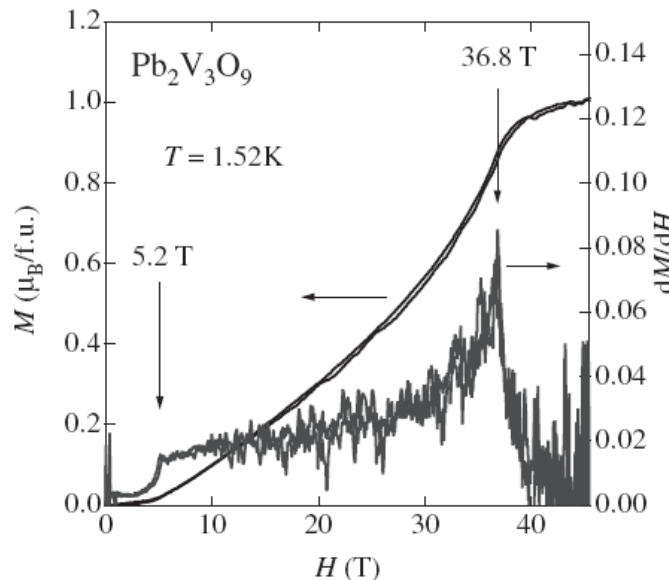
Figure 5 Evolution of the magnetization of $Pb_2V_3O_9$ in high fields, indicating a transition at the spin gap (5.2 T) and continued growth until 36.8 T (ref. 17).

There are also examples of spin-1/2 chains (the Majumdar Ghosh model) that have yet to be explored experimentally, where there unbound spinons have been predicted above a finite gap in the excitation spectrum[18].

To better understand these and other distinct cooperative states in one dimensional quantum systems, it is essential to explore the transition between them. This is possible

through the application of a sufficiently large magnetic field to a spin system with a gapped excitation spectrum. For the spin-1 chain the transition should to take place through a Bose condensation of magnons followed by the formation of a critical state with unbound spinons in the high field limit[19]. While there should be similarities with the critical state of the spin-1/2 chain, different dynamical critical exponents should reveal a different Luttinger Liquid phase. While such high field experiments have been attempted, they have not yet been successful in revealing a field induced quantum critical state. For spin-1 chains the problem is single ion anisotropies, which when combined with a field perpendicular to the spin chain lead to an Ising state rather than a gapless critical phase. For spin-1/2 systems with a zero field gap the problem so far has been that the energy scales for materials where the gap can be closed with current magnet systems are too small for effective inelastic neutron scattering experiments[20].

Another set of interesting low dimensional systems are ones that undergo a Spin-Peierls Transition. In these materials it is energetically favorable for the spin chains to be uniform at high temperatures and then with decreasing temperature to distort into alternating chains. The compounds TiOCl and TiOBr are the first examples of inorganic compounds beyond $CuGeO_3$ which show what this type of lattice distortion.[21] The chemical structure of TiOX (X= Cl, Br) is such that there are insolated, one-dimensional chains of Ti^{3+} spins throughout the lattice.[22,23] These chains cannot interact magnetically with other chains (or more precisely, the interactions are extremely weak), because of the bonding within the solid. Ti^{3+} in this environment has one unpaired electron, and because of this, quantum effects are very significant. For 1D systems with these spin configurations, a transition is predicted to occur at low temperatures where the spins "pair up" into up/down orientations (a Spin-Peierls distortion). As a result of this, the lattice distorts to form dimers along each chain, and a spin-gap develops. The inelastic neutron spectra of $CuGeO_3$ ($T_{SP} \sim 14$ K) has been measured in fields up to 10 T to investigate the nature of the spin gap. TiOCl and TiOBr have energy scales which are roughly an order of magnitude larger than $CuGeO_3$, so larger magnetic fields are needed to make a comparision study. A beamline which has the capability to reach 35 T would allow the exploration of the spin dynamics in high fields to test against theoretical predictions of the spin gap.

All of these issues could be overcome with a >30 T magnet that applies the field along the chain direction and allow inelastic neutron scattering experiments with wave vector transfer along the spin chain and field direction. Spin-1 systems with near easy plane symmetry such as NDMAP[14] and NENP[12] could then be driven deeply into the high field easy plane state to explore spinon continuum scattering there. For gapped spin-1/2 systems it would be possible to enter the high field critical state for a wider range of structurally and spontaneously dimerized spin-1/2 chain systems where the energy scales are amenable for inelastic neutrons scattering experiments[24]. Other experiments that would be enabled by high fields and neutrons scattering are experiments that probe the relationship between bound states and continua as a function of the field tuned gap[25,26] and experiments that probe quantum impurities as a function of the quantum length scale that is implied by the spin gap[16]. Each of these experiments could have a profound impact

on our understanding of quantum many body physics in one dimension and more generally on our understanding of strong correlations in quantum systems.

2.1.1.3 Two dimensional Magnetism

Interested Participants: Collin Broholm, Mechtilde Enderle, Garrett Granroth, Bella Lake, Mark Lumsden, Igor Zaliznyak
Other Interested Researchers: Martin Greven (Stanford University), Andrey Zheludev (Oak Ridge National Laboratory)

Two is the lower critical dimensionality for order among spins with a continuous degree of freedom. It is also the interface dimensionality for our three dimensional world. As a result, there is much interesting physics in two dimensions and a potential that a better understanding of cooperative effects in two dimensions could have impact in other fields of science and technology. Again insulating quantum magnets are ideal model systems and neutron scattering experiments in high magnetic fields are essential for progress.

Lamellar spin systems with competing interactions are of particular interest as conventional magnetic order can be suppressed even at T=0. Figure 6a shows a particularly simple example of a planar system formed by spin-1/2 degree of freedom on the vertexes of triangles[27,28]. The magnetization plateau in Figure 6b indicates that there is a high field state where the triangles are magnetized to one Bohr magneton each and the excitation spectrum is gapped.
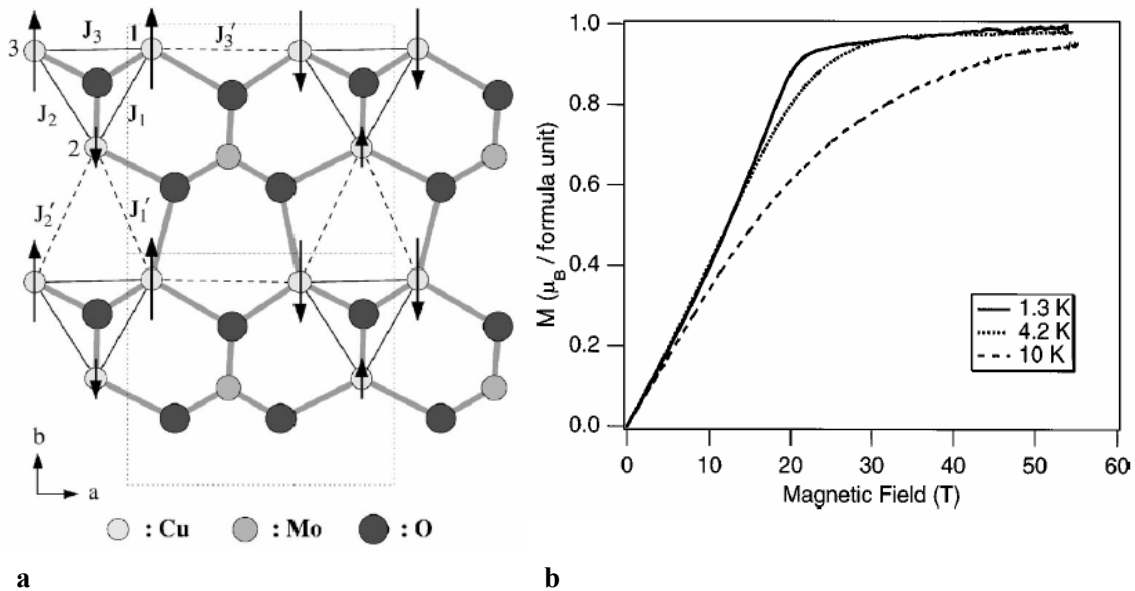
Figure 6 (a) Planar structure of a $La_4Cu_3MoO_{12}$, which contains interacting spin-1/2 trimers[25]. (b) Magnetization Plateau caused by the interactions of these trimers (Ref. 6). Neutron diffraction is needed to determine the high field spin state but cannot be performed on present day instrumentation.

The combination of neutron diffraction experiments to resolve the ordered structure in the high field phase and inelastic neutron scattering to establish the microscopic nature of the dimerized state are required for a comprehensive understanding of this unique correlated quantum state.

The Kagomé lattice antiferromagnet has remarkable cooperative properties that are only now beginning to be explored experimentally. For Ising spins there is no phase transition and the correlation length remains short in the T=0 limit[29]. For spin-1/2 exact numerical diagonalization of small clusters indicate that there is an isolated singlet ground state with a small energy gap to a high density of singlet states[30]. Model systems available so far have glassy low temperature phases where quenched disorder of various sorts may obscure interesting physics associated with a gapless spin liquid[31]. Upon application of high magnetic fields the spin-glass like transitions, however, have been found to be suppressed[32] and this raises the possibility that the interesting high field physics of the kagomé lattice may be accessible in some of these materials. Several high field phases have been predicted[31] for the kagomé antiferromagnet as indicated in Figure 7.
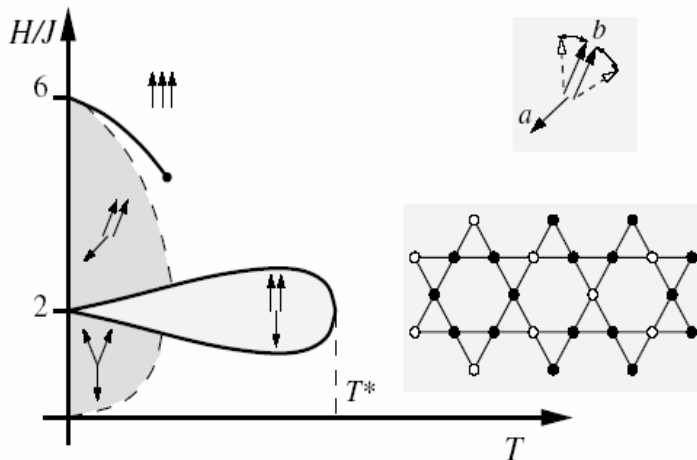
.
Figure 7 Schematic high magnetic field phase diagram predicted for the kagomé lattice antiferromagnet. From (Ref. 7).

Information from magnetic neutron scattering on spin correlations in such phases would be important for progress in understanding the intricate many body physics of the kagomé lattice. In providing an essential new dimension through which to explore near quantum critical two dimensional spin systems, a high field magnet for neutron scattering to accelerate experimental identification of a gapless spin liquid in two dimensional.

$SrCu_2(BO_3)_2$ is a remarkable example of two dimensional magnet that realizes a spin-1/2 two dimensional magnet with an exactly known many body ground state[33]. The lattice consists of spin-1/2 dimers with strong but frustrated inter-dimer interactions. The frustration is so effective in suppressing triplet hopping amplitudes that there is little detectable dispersion in the zero field neutron scattering spectra[34]. In fact this makes it quite difficult to extract information about the actual spin Hamiltonian for this material. High field magnetization experiments[35] reproduced in Figure 8. however, show that

qualitatively different quantum phases can be induced through the application of high magnetic fields. Again high fields provide access to entirely different quantum many body phases the detailed microscopic characterization of which will help to establish the spin Hamiltonian of $SrCu_2(BO_3)_2$ and more importantly will contribute to the task of classifying what types of correlated quantum states are possible in two dimensional systems with short range interactions. In addition, it is also of great interest to characterize the dynamic and static critical exponents associated with the phase transitions between these different states of matter.
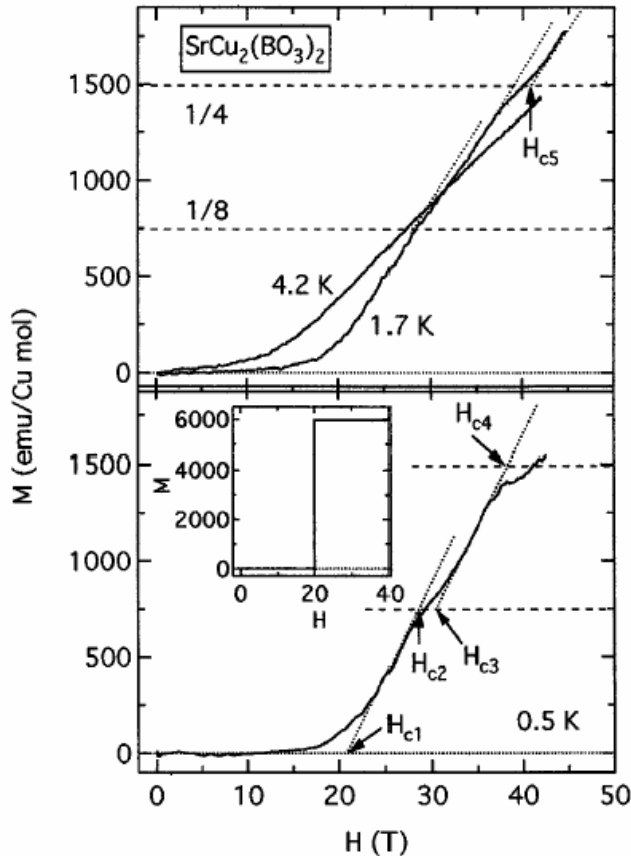
Figure 8 Magnetization curve for the frustrated 2D coupled dimer compound $SrCu_2(BO_3)_2$ (ref. [31]). Neutron scattering is needed to understand the microscopic nature of the plateau phases.

2.1.1.4 Topological magnetization plateau phases

A number of quantum magnets of various dimensionality demonstrate the phenomenon of topological quantization of macroscopic magnetization that is strikingly analogous to the quantum Hall effect[36,37]. The manifestation are extended plateaus in the magnetization curves m(H) that occur at integer or rational-fraction values of total magnetization per site. Within the range of each magnetization plateau the system retains a commensurate magnetic structure, and the excitation spectrum is gapped. As the end of each plateau is reached by increasing the external magnetic field, the spin gap closes. At this point the magnetic structure becomes incommensurate, and, with increasing field, continuously morphs into the stable commensurate state of the next plateau. Once this consecutive stable commensurate state is reached, the gap re-opens.
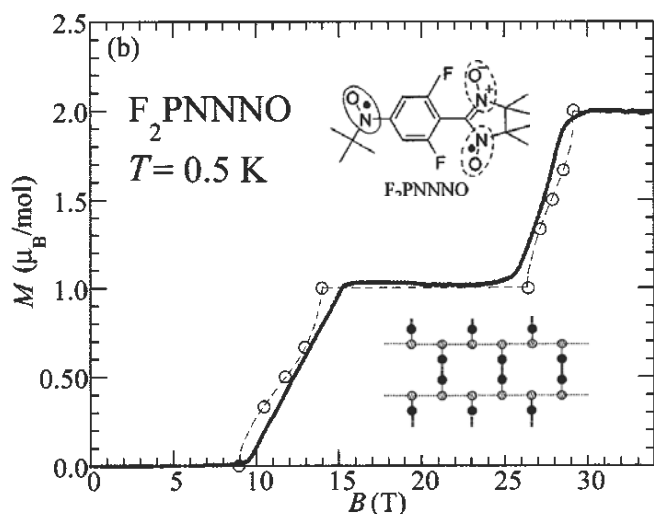
Figure 9 The magnetization curve of F_2PNNNO shows a clear plateau at *m=1*

Magnetization plateaus, both integer and rational, have been observed in several magnetic materials. Examples include the S=1/2 dimer system NH_4CuCl_3 with plateaus at m=*1/4* and m=*3/4* (ref. 38), the S=1/2 spin ladder system $(C_5H_{12}N)_2CuBr_4$ with an plateau at m=1/2 (ref. 39), the above-mentioned 2-dimensional S=1/2 system $SrCu_2(BO_3)_2$ with *m=1/8*, *m=1/4* and *m=1/3* plateaus, the quasi-2D frustrated S=1/2 system Cs_2CuBr_4 (m=1/3 plateau)[40], S=1 dimer compound $Ba_3Mn_2O_8$ (*m=1*) (ref. 41), the above-mentioned S=1 bond-alternating chain NTENP (*m=1*) (ref. 42). Neutron scattering is the tool of choice for investigating of the magnetic structures of the plateau and inter-plateau states, as well as the exotic magnetic excitations expected in these phases. Unfortunately, with the exception of NH_4CuCl_3 (ref. 43) and $(C_5H_{12}N)_2CuBr_4$ (ref. 39), in all known model materials even the first plateau occurs in magnetic fields of over 20 T, and is therefore at present inaccessible to such studies. Provided that magnetic fields in excess of 15 T will become available for neutron scattering experiments, a very interesting model system for the study of plateau states could be the purely organic quantum antiferromagnet F_2PNNO (ref 44.) This molecular biradical crystallizes to form a quasi-2D network with a spin gap of ~1 meV. An *m=1* plateau state extends from H=15 T to H=25 T (Figure 9). It will be of great interest to determine the spin arrangement below, on, above this extended gapped phase, and to study the spin excitation spectrum.

2.1.1.5 Frustrated Magnetism

Interested Participants: Collin Broholm, Garrett Granroth, Seung-Hun Lee, Young Lee, Mark Lumsden
Other Interested Researchers: Bruce Gaulin (McMaster University), Christopher Wiebe(Florida State University)

An alternate route to unconventional magnetism in insulators is magnetic frustration. Consider a square of spins with antiferromagnetic interactions. Apart from global spin rotation symmetry there is a single well defined classical spin configuration that satisfies all near neighbor antiferromagnetic interactions. However, if diagonal interactions of equal strength are added it is no longer possible to fully satisfy all interactions simultaneously. Instead of a single low energy spin configuration, there is now a two dimensional continuous manifold of states with the same classical energy[45]. The square with crossings has the connectivity and symmetry of spins on the vertices of a tetrahedron so this type of geometrically frustrated system is a common motif in cubic solids. Understanding how such symmetry induced degeneracies are lifted as a result of quantum fluctuations and sub-leading interactions is a very active area of condensed matter research. One of the attractions of this field is that powerful microscopic probes of correlations such as neutron scattering are available, which is not the case for related strongly correlated systems such as quantum Hall semiconductor hetero structures.

An interesting consequence of geometrical frustration in antiferromagnets is that these materials can be remarkably insensitive to magnetic fields at low temperatures. The implication is that leading interactions in frustrated antiferromagnets define a non-magnetic low energy manifold much as in the Haldane spin-1 chain described in Section 2.1.1.2. In the spinel and pyrochlore antiferromagnets this manifold is thought to be associated with states built from non-magnetic tetrahedral spin clusters[46]. Indeed neutron scattering experiments directly verify through the absence of scattering in the low Q limit that dipole moments are locally screened in these systems. Coherent diffuse magnetic neutron scattering also indicates that spins form composite degrees of freedom in these systems. However, it is at present unclear whether this can become a robust description of frustrated magnets or whether the match between neutron diffraction patterns and the Fourier transform of certain discrete spin clusters could be a coincident result of the short two-point correlation lengths in these systems.

Frustrated magnets are also interesting materials to probe aspects of spin chirality: both vector chirality and scalar chirality. The Kagome lattice material, the iron jarosite $KFe_3(OH)_6(SO_4)_2$, possesses robust chiral correlations related to the arrangement of spins around triangular plaquettes. The presence of spin chirality in condensed matter systems may play a role in important phenomena ranging from high-T_C superconductivity to the anomalous Hall effect. Currently, there are relatively few experimental studies of spin chirality in frustrated magnets. Lee and coworkers have discovered a field-induced spin-canting transition which corresponds to a non-trivial change in the spin-texture of the jarosite sample. In particular, the transition yields a net, non-zero value for the scalar chirality. For $H < H_C$ (where H_C may be as large as ~30 T at low temperatures), the net scalar chirality for our jarosite sample is zero because the contributions from neighboring planes are equal and opposite. However, for $H > H_C$ the spins flip by 180 degrees and the net scalar chirality becomes non-zero. There are few materials with non-zero scalar chirality in the ordered state, especially on a two-dimensional lattice. In iron jarosite, a phase transition occurs in which a net scalar chirality can be "switched on" by a magnetic field. It would be interesting to gather more detailed microscopic information by

studying both the vector and scalar chirality correlations in high fields with x-rays and neutrons

High magnetic field experiments will likely be key to developing a comprehensive understanding of these complex materials. Indeed, high field experiments have already shown interesting magnetization plateaus both in spinel[47] and pyrochlore spin ice systems. However, in the antiferromagnetic spinel systems, the high field scales for these plateaus have precluded neutron scattering experiments to determine the microscopic correlations of the plateau phases. Such experiments on oxides to fields of order 35 Tesla would both provide valuable input towards establishing the microscopic models for specific materials but also and more importantly they should enable detailed microscopic characterization of multiple degenerate manifolds in individual frustrated material as a function of the applied field.
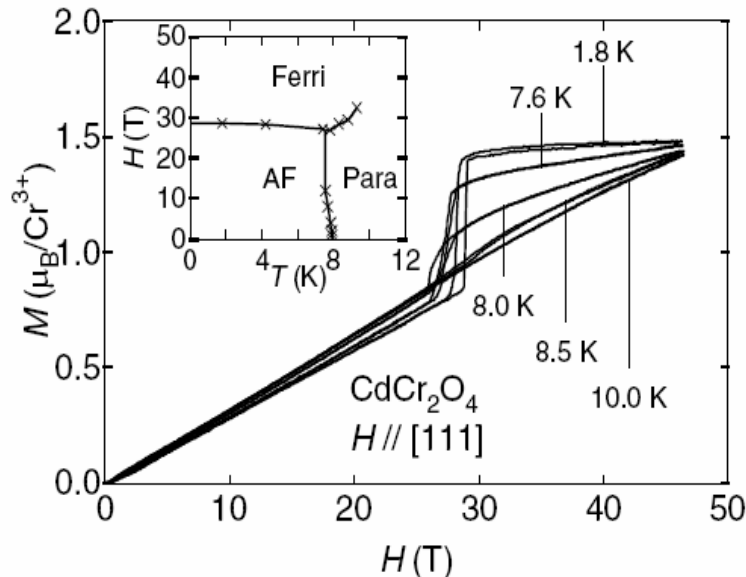
Figure 10 Field dependence of magnetization of $CdCr_2O_4$ showing a clear magnetization plateau for H>28 T. Reproduced from (ref. 5)

A specific example is provided by the material $CdCr_2O_4$ (ref. 47). This compound contains spin-3/2 degrees of freedom on the vertexes of corner-sharing tetrahedra. In zero field there is an interesting low temperature state where it appears that a lattice distortion enables spin order in a Jahn-Teller like phase transition. Figure 10 shows that in a field of approximately 28 Tesla, there is a transition to a ferrimagnetic phase with a much smaller differential susceptibility[47]. The magnetization plateau suggests a gapped high field phase. Both spectroscopic and structural information such as can be obtained from neutron scattering are needed to understand the transition and the nature of the high field phase. The ability to explore microscopic correlations in two zero temperature cooperative phases of the same material could produce a breakthrough in our understanding of geometrical frustration in materials science.

Another example is $Tb_2Ti_2O_7$, a pyrochlore with a network of Tb^{3+} spins on corner-shared tetrahedra.[48] This system has a spin-liquid ground state, where the spins cannot order at low temperatures and remain paramagnetic. However, by applying a magnetic field, a rich phase diagram of different ordered states develops. This phase diagram is still being elucidated, with some evidence suggesting that the system does not find a completely ordered state until a field of ~18 T is reached[49]. Materials such as these would be prime candidates for further study using a high-field neutron beamline.
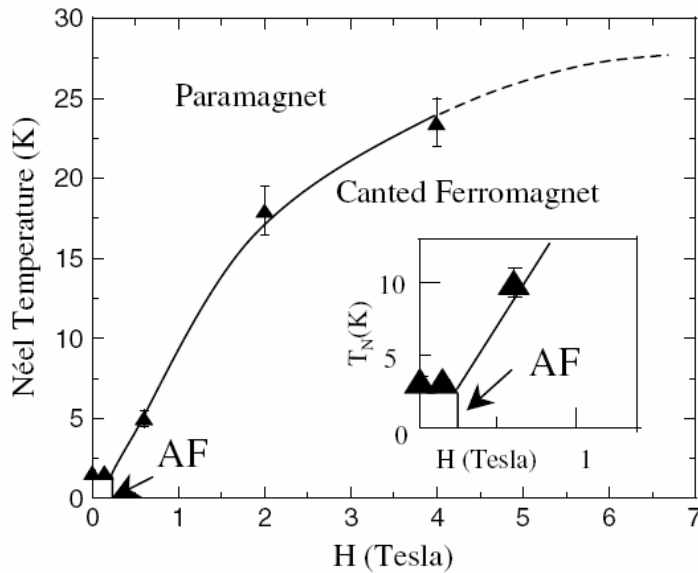
Figure 11 Phase diagram of $Tb_2Ti_2O_7$ (from (Ref. 49)). There is continued evolution of the Néel Temperature of the ordered state up to very high fields.

Recently, there are considerable activities in studying geometrically spin frustrated systems because of their rich ground states including ferroelectric phases[50,51,52]. It is believed that there is significant coupling between two disparate order parameter of antiferromagnetism (AFM) and ferroelectricity (FE)[53]. The triangular lattice antiferromagnetic (TLA), in which magnetic ions reside at a triangular network, is the most obvious example of a geometrically frustrated magnetic system. As a prototype model for TLA system, $CuFeO_2$ has layered structure of triangular lattice of Fe^{3+} ions, each triangular layer is separated by non-magnetic Cu^{1+} and O^{2-} layers and stacks along c axis (Figure 12). Previous neutron scattering diffraction measurement suggested that $CuFeO_2$ has unique magnetic properties where a collinear commensurate 4-sublattice magnetic structure ($\uparrow\uparrow\downarrow\downarrow$) [collinear-CM(1/4)] forms within the Fe^{3+} plane in zero magnetic field.

One of the most intriguing features of $CuFeO_2$ is the evolution of its magnetic properties when a magnetic field B is applied along the c axis. Magnetic phase diagram revealed by measurements of magnetization, dielectric constant, electric polarization, and magnetostriction suggests exotic ground states in the field (Figure 12). A field between

19

13 and 20 Tesla will induce another collinear-CM(1/5) phase in which the spin moments along the c axis in each layer exhibit the (↑↑↑↓↓) configuration. Between the collinear-CM(1/4) and collinear-CM(1/5) phase (field between 7 and 13 T), there exists the first B-induced noncollinear spin structure state. Recent magnetostriction measurement on the $CuFeO_2$ single crystal indicates such noncollinear spin structure plays a key role in inducing electric polarization and suggests that the frustrated magnets are likely the candidates for multiferroics materials with strong magnetoelectric interactions. Among the multiferroics studied to date, it is known that there exists a strong coupling between magnetism and ferroelectricity as well as long-range magnetic structures. Synchrotron X-ray studies on one compound $TbMnO_3$ reveal the appearance of lattice distortion with non-zero propagation wave-vector and its lock-in transition is accompanied by the spontaneous ferroelectric order[54]. Neutron scattering on other magnetic frustrated compound like $TbMn_2O_5$ further suggest a strong coupling between the structural anomaly and multiferroics behavior[55]. To model the interaction between ferroelectric and magnetic order in $CuFeO_2$ in its nonconllinear spin state, we need to carry out elastic and inelastic neutron scattering in the field above 15 Tesla, which would greatly benefit from the proposed high field magnet.
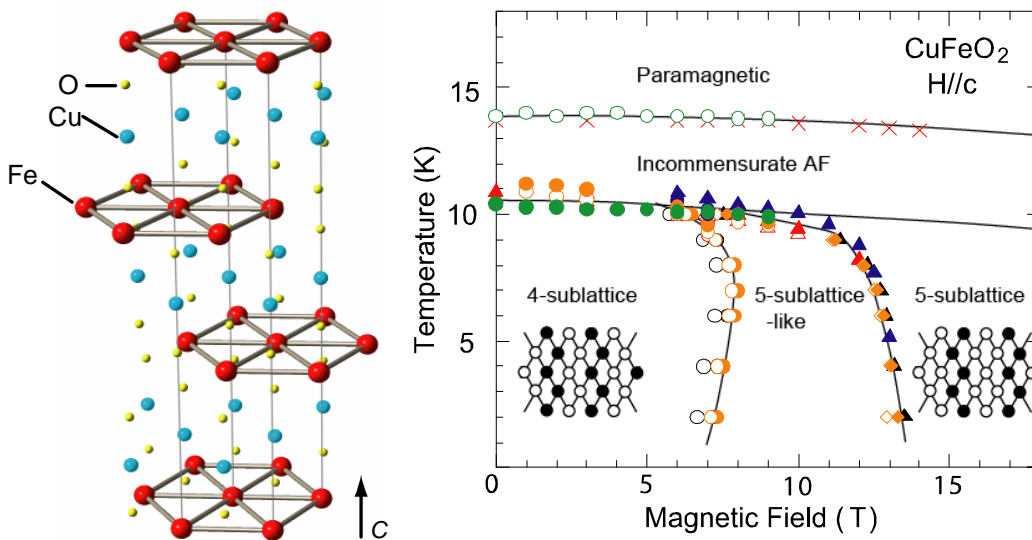
Figure 12 Crystal structure of $CuFeO_2$ and its general phase diagram of in the temperature-field plane.

2.1.2 Measuring the Spin Hamiltonian with High Magnetic Field

Ineterested Participants: Collin Broholm, Mechtilde Enderle, Garrett Granroth, Bella Lake, Seung – Hun Lee, Mark Lumsden, James Rhyne, Igor Zaliznyak,
Other Interested Researchers: Andrey Zheludev

A key ingredient to the past impact scientific work on insulating magnetic systems is the close connection between theory and experiments that was possible through a well defined microscopic description of interactions in a spin Hamiltonian[1]. For simple

systems where there is only a single relevant exchange constant the spin Hamiltonian can readily be determined through bulk experiments. However, in more complex materials where several exchange constants, their anisotropy, as well as single ion anisotropy terms are important, it is not possible to extract this information say from high temperature susceptibility measurements alone. The problem is compounded by the fact that dynamic properties measured by inelastic neutron scattering can be described as "emergent" in that relating them back to the microscopic interactions is a significant theoretical challenge.

A solution for this problem was developed in the context of experiments on $CsCuCl_4$ where it was crucial to have reliable model independent information about the spin Hamiltonian and its anisotropies[56]. This was obtained by driving the system into a ferromagnetic state where the ground and excited states are known exactly for all possible forms of spin Hamiltonians. Rather than "emergent properties", there are only magnons associated with each of the collective modes of the interacting spin system. By measuring and fitting ferromagnetic spin wave dispersion relations, it was possible to extract accurate information about the spin Hamiltonian without any dubious assumptions[56].

By expanding the accessible field scale from 15 T at present to more than 30 T, a definitive determination of the spin Hamiltonian will be possible in a much wider range of interesting quantum magnets. Specific examples include CDC, which is a spin-1/2 chain system with an alternating g-tensor and Dzyaloshinskii-Moriya interactions (See Fig. 1) and PHCC, which is a two dimensional frustrated quantum magnet with an isolated singlet ground state[57]. The determination of the spin Hamiltonian for these materials at present requires use of the very theory that one is trying to evaluate. Ferromagnetic spin wave measurements in the high field phase would raise the debate between theory and experiment to a more stringent and productive level.

2.1.3 Characteristics of neutron Instrumentation required for insulating magnetic systems

The primary instrumentation objective should be to enable neutron scattering experiments in significantly higher field than was previously possible. An attractive and seemingly achievable goal would be 35 Tesla. In the scientific area of quantum magnetism, such a magnet would open up an important new class of experiments that are impossible with present day magnet systems. The superconducting hybrid technology makes such a magnet technically feasible and relatively economic to operate. The enhanced brightness of the Spallation Neutron Source will enable a wide range of neutron scattering experiments even under the restrictive conditions that are necessary to reach fields in excess of 30 Tesla.

Because the magnet will be unique, the neutron scattering instrumentation must be correspondingly versatile to take advantage of the unique thermodynamic conditions. The neutron instrumentation should enable comprehensive single crystal magnetic and chemical structure refinement. Polarized neutron capabilities would be helpful but not essential for this work. Inelastic scattering forms an essential part of the scientific program. An important energy range is that defined by the Zeeman energy splitting for

an electronic spin in the applied field, which is approximately 4 meV in 35 Tesla. However, higher energies are also needed when as for example in $SrCu_2(BO_3)_2$ the ground state is profoundly modified by the field. In that case selection rules will modify the spectrum over the full bandwidth that over the class of systems of importance extends as high as 50 meV. For experiments that probe field induced gapless spin systems low temperatures ($\approx$50 mK) and high energy resolution ($\approx$0.1 meV) is needed. At higher energy transfer 5% energy resolution will typically be adequate.

Rotation of the sample with respect to the direction of the incident beam will be necessary. The minimal requirement would be full rotation about a direction perpendicular to the incident beam. Smaller adjustments of $\pm10^o$ about directions perpendicular to the principal direction of this rotation would be helpful too. Sample dimensions will vary from 1 mm^3 to several cm^3. Temperature requirements are 50 mK to 300 K. There will be a need for accurate and rapid temperature control when mapping H-T phase diagrams. This may necessitate a range of cooling technologies from dilution fridge, through pumped ^{3}He and ^{4}He to flow cryostats and displex systems. As the sample and signal will be small there will be a need to reduce scattering contributions from the magnet and sample environment system. This will require optimized incident beam focusing as well as effective shielding of the sample area with neutron absorbing materials.

2.1.4 Conclusions for high magnetic field studies of insulating magnets

Neutron scattering experiments on low dimensional and frustrated quantum magnets are providing important new information on the combined effects of quantum mechanics and strong correlations in many body systems. Progress in this field of science is frequently gated by what types of model systems are available for experiments and by how well it is possible to know the underlying microscopic spin Hamiltonian. On both of these counts high magnetic field experiments would have an important impact. By applying a large field to an insulating quantum magnet the same material can realize a range of different cooperative states and in doing so also provide access to the intervening quantum phase transitions. When only the field varies between these states, it is possible to extract information about the underlying spin Hamiltonian from the state where this is done most easily based on inelastic neutron scattering data. Typically this may be the fully magnetized state though it could also be more conventional transverse Néel ordered states for systems that cannot be fully polarized. The highest priority for instrumentation is to maximize the magnetic field, provide a flexible diffractometer for single crystal magnetic structure refinement, a flexible spectrometer for the energy range 0-50 meV with resolution 0.1 meV or 5% of $\hbar\omega$, and provide a wide and rapidly accessible temperature range with accurate control from 0.05 K to 300 K.

2.2 Systems with Conduction electrons

2.2.1 High Temperature Superconductors

Interested Participants: Bella Lake, Gabe Aeppli, Pengcheng Dai, Valery Kiryukhin, Young Lee, Jorg Strempfer, and Zahirul Islam

Other Interested Researchers: Bruce Gaulin (McMaster University), Martin Greven (Stanford University)

Cuprate high-temperature superconductivity is a central unsolved problem in condensed matter physics. Materials such as $La_{2-x}Sr_xCuO_4$, La_2CuO_{4+y}, $Bi_2Sr_2CaCu_2O_{8+\delta}$ and $YBa_2Cu_3O_{6+x}$ are derived from insulating antiferromagnets via hole doping and can be superconducting up to temperatures of 165K. While the mechanism driving high-temperature superconductivity is not yet understood there is considerable speculation that the pairing mechanism may be of magnetic origin. Neutron scattering has made a considerable contribution to our understanding of high temperature superconductivity. This is because neutron magnetic scattering can determine the energy and momentum dependence of the imaginary part of the dynamical susceptibility ($\chi"(Q,\omega)$), providing information crucial in addressing the relationship between magnetism and superconductivity. Experiments reveal the presence of incommensurate magnetic order and magnetic fluctuations co-existing with superconductivity.   The interplay of magnetism and superconducticity has also been studied with a suppression of the magnetism in the superconducting phase observed below a spin gap (analogous to the energy gap arising from charge pairing), and the sharpening of a resonance in the some high-T_c materials. Neutron scattering using high magnetic fields is of central importance because the applied field interacts not only with the magnetism but also with the superconductivity.
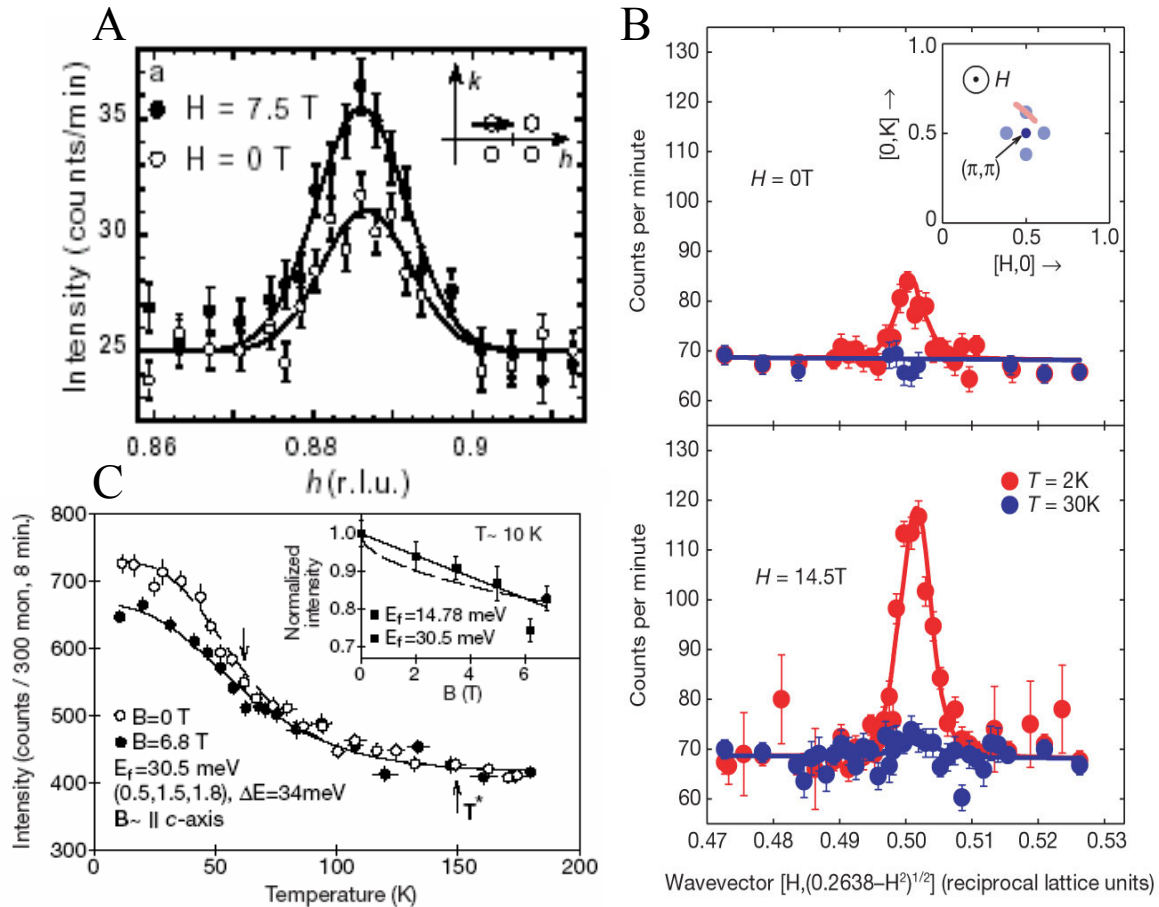
Figure 13 Field-induced magnetic order in (A) La$_2$CuO$_{4+y}$ and (B) La$_{2-x}$Sr$_x$CuO$_4$, and (C) field-induced suppression of the resonance in YBa$_2$Cu$_3$O$_{6+x}$

An experiment that is crucial to our understanding of high-T_c materials is the determination of the physical state of the material when superconductivity is eliminated by an applied magnetic field. This would allow determination of the physical properties of these materials in the absence of superconductivity and supplying information about the ground state that would have occurred if superconductivity had not intervened, thus providing a starting point for theory. However, upper critical fields required to suppress superconductivity in hole-doped high-T_c materials are greater than 30T. As a consequence, an investigation of the magnetism in the high field phase has not so far been possible. To date neutron scattering experiments can be done with fields of up to 15T and already these have revealed interesting phenomena in high-Tc materials. Among the results are enhanced magnetic fluctuation within the spin-gap of optimally-doped and overdoped La$_{2-x}$Sr$_x$CuO$_4$ (ref.58,59), field-induced magnetic order in underdoped La$_{2-x}$Sr$_x$CuO$_4$ (ref. 60) and La$_2$CuO$_{4+y}$ (ref. 61) and a reduction of the magnetic resonance of YBa$_2$Cu$_3$O$_{6+x}$ (ref. 62). These findings suggest that as superconductivity is suppressed by applied fields the magnetism also evolves - a result that raises many questions, e.g. what is the physical state in La$_{2-x}$Sr$_x$CuO$_4$, and La$_2$CuO$_{4+y}$ for field greater than the upper critical field are they incommensurate antiferromagnets? What about YBa$_2$Cu$_3$O$_{6+x}$, where field-induced magnetic ordering has not been observed with available fields? What is the role of the resonance in YBa$_2$Cu$_3$O$_{6+x}$ will it continue to decrease with field

24

and at what field will it disappear? For optimally doped superconductors the size of the fields required are greater than 60T, but already a considerable part of the high field phase diagram can be explored (using underdoped and overdoped materials) with a 40T field, thus the proposed 40T magnet will allow these highly important questions to be answered.

Beams of X-rays with APS intensities are also crucial for observing the charge order in the High-T_c compounds.

2.2.2 Colossal Magnetoresistance (CMR) materials

Intersted Participants : Pengcheng Dai

The manganese oxides with general composition $R_{1-x}A_x$MnO$_3$ (R and A are trivalent rare-earth ions and divalent alkaline-earth ions, respectively) have been actively investigated over the past decades because of the colossal magnetoresistance (CMR) effect observed around x~0.30. The parent compounds RMnO$_3$ are Mott insulators, and the Mn^{3+} ions have an electron configuration $t_{2g}^3 e_g^1$ (S=2). Substitution of R^{3+} with A^{2+} introduces holes in the e_g orbital and causes an insulator-metal transition. For example, in La$_{1-x}$Sr$_x$MnO$_3$ with x above 0.17, a metallic ferromagnet is formed due to the double exchange (DE) interaction and CMR effect is observed around the Curie temperature. This CMR effect has been explained in terms of the strong on-site Hund's rule coupling between localized spins S=3/2 in the t_{2g} orbital and itinerant carriers in the e_g orbital which facilitate both ferromagnetism and electrical conductivity. In some of the $R_{1-x}A_x$MnO$_3$ systems with the ionic radii for the R and A sites being relatively small, however, the hole-doping does not produce the ferromagnetic metallic state. Instead, a charge and orbital ordered (CO-OO) states appears[63].

The CO state of the CMR perovskite manganites is one of the most interesting and important phenomenon. Since the charge ordering is usually accompanied by the orbital ordering, and some times by the very peculiar zigzag antiferromagnetic (AFM) ordering. There are significant experimental evidences for the existence of a fundamental connection between the CO-OO phenomenon and the AFM spin ordering. Elastic neutron scattering measurement in Pr$_{0.7}$Ca$_{0.3}$MnO$_3$ suggested the collapse of the CO-OO state under external magnetic fields. When the insulator-to-metal (I-M) transition is induced by magnetic field, there is a discontinuous change in the spin-wave stiffness constant D (Figure 14c)[64]. This result implies that the I-M transition is not achieved by the simple percolation of micron-sized metallic clusters as currently believed, but involves a first-order transformation. These findings suggest a drastic change in spin interactions as magnetic field tuned the sample from an insulator to metal. Unfortunately, the available magnet facility (<11Tesla) would only allow the studies of material with lower critical field, where phase coexistence usually takes place. For carrier doping x close to 0.5, the stable and single phase of CO-OO state might persist up to H = 25 Tesla for Pr$_{0.5}$Ca$_{0.5}$MnO$_3$ at low temperature (Figure 14a). A better understanding of the interplay between spin, lattice, electron and orbital degrees of freedom requires a higher magnetic field. The proposed 40 Tesla would address those issues directly.
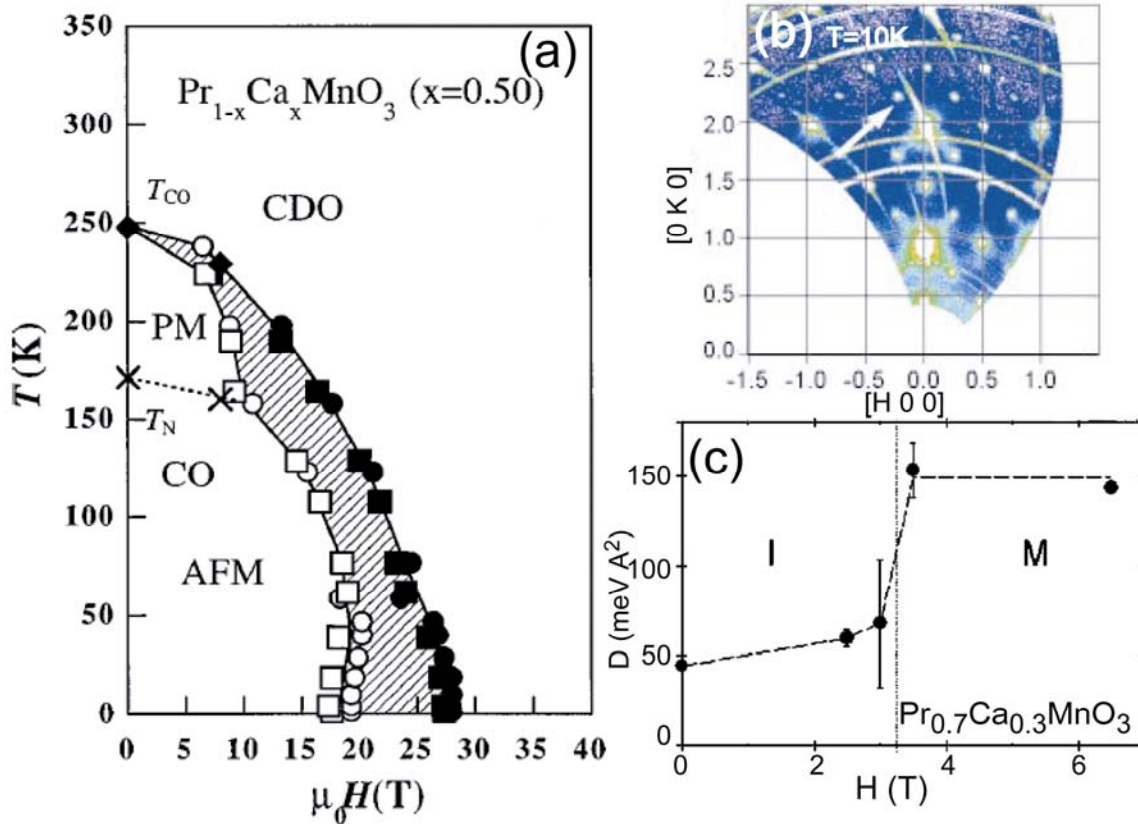
Figure 14 (a) Phase diagram in the H-T plane of $Pr_{0.5}Ca_{0.5}MnO_3$ determined by M and MR measurement[63]. (b) CE-type charge/orbital ordering in $Pr_{0.7}Ca_{0.3}MnO_3$ in zero magnetic field[64] . (c) Discontinuous change of spin-wave stiffness induced by magnetic field underlies first-order transition of microscopic magnetic interactions[64].

2.2.3 Multiferroics

Recently discovered Mn-based multiferroic compounds ($ReMnO_3$, $ReMn_2O_5$) have generated a lot of interest. In these materials magnetization and electric polarization are intricately coupled. Both the details of magnetic structure and atomic displacements need to be studied in fields up to 30 Tesla to reveal the origin of ferroelectricity on these materials. Several researchers, in particular T. Kimura, discussed bulk measurements and structural studies of various compounds in this class.

The magnetoelectric effect involves the induction of magnetization by means of an electric field and induction of polarization by means of a magnetic field. From a technological point of view, the mutual control of electric and magnetic properties is an attractive possibility, but the limited number of candidate materials and the smallness of the observed effects have tempered excitement in this area. The recent observation of gigantic magnetoelectric and magnetocapacitive properties in rare-earth manganites, $TbMnO_3$ and $DyMnO_3$ (refs. 65,66) however, has renewed interest in these effects. Ferroelectricity in these materials appears to originate from the competing magnetic

interactions that cause lattice modulations through magnetoelastic coupling. High-resolution x-ray scattering provides an ideal tool for measuring this coupling between the structural and magnetic order. Preliminary studies have already shown the presence of magnetoelectirc phases in fields up to 9 Tesla. Magnetoelectric transitions at even higher fields are expected in these and other materials.

2.2.4 Cobalt oxides

Interested Participants: Young Lee, Mark Lumsden, Pengcheng Dai

The study of spin fluctuations in a novel interesting superconductor Na_xCoO_2 (also a SDW / CDW system) would greatly benefit from the availability of 40 T field. Y.S. Lee discussed further this fascinating compound.

Sodium cobalt oxide, Na_xCoO_2 (x ~ 0.65 to 0.75), has received considerable attention due to its unusual thermal electric properties.[67] Recent studies have revealed anomalous non-Fermi liquid behavior in transport properties which point to the importance of strong correlation.[68,69] The structure consists of CoO_2 layers separated from each other by Na layers, as shown in Figure 1. The cobalt ions form a two-dimensional triangular lattice. By varying the Na content, the average valence of the Co ions may be altered; the formally *1-x* fraction is in the low spin (S=1/2) Co^{4+} state, while the *x* fraction is in the S=0 Co^{3+} state. Interest in this material escalated with the discovery of superconductivity by Takada et al.[70] in $Na_xCoO_2 + yH_2O$ when the sodium concentration is reduced to about 0.3 and water is intercalated between the layers. The ability to control the sodium content is an exciting development because, in principle, the limit of *x=0* corresponds to a Mott insulator on a triangular lattice with S=1/2. Then the hydrated compound can be viewed as electron doping of a Mott insulator with a doping concentration x ~ 0.3. As such, it is the second known example of superconductivity arising from doping a Mott insulator after the high T_C cuprates.

Most of the initial studies on the superconducting compound have been performed on powder samples. Based on the limited available literature on Na_xCoO_2 crystal growth, crystal sizes appear limited to about 1 mm in dimension using the low temperature slow cooling method with NaCl as a flux.[71] There has been recent success in producing single crystal samples.[72] Lee and coworkers have recently
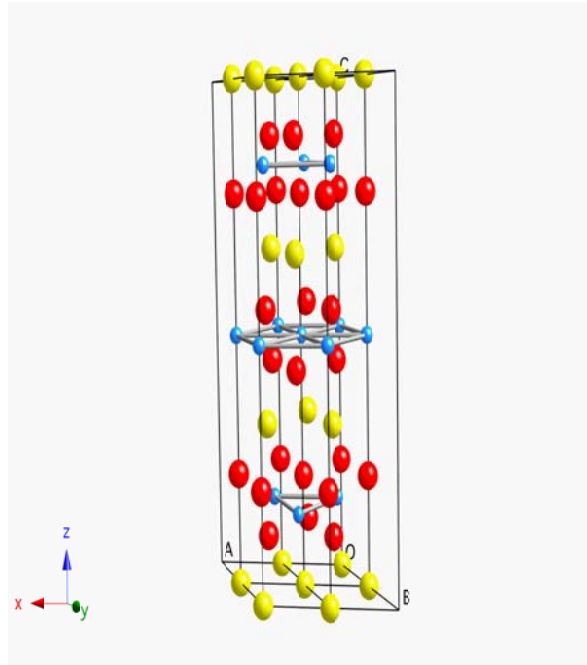
Figure 15 Crystal structure of NaCoO₂. The Co ions (small spheres) form a triangular lattice and are surrounded by oxygen atoms in an octahedral arrangement. The Na ions lie in a plane between these CoO₂ layers.

begun an effort to extract Na from large Na_xCoO_2 single crystals using an electrochemical deintercalation technique[73] which is an alternative to the chemical de-intercalation of Na using Br ions introduced by Takada.[70] The electrochemical method permits precise control of the Na content, and, in addition, it has allowed for the production of large single crystals of $Na_xCoO_2 \cdot yH_2O$ suitable for neutron scattering and x-ray scattering measurements.

By studying the spin fluctuations in the hydrated superconductor with neutron scattering, one can probe the interplay between the magnetism and the superconductivity. Applying a magnetic field can be used to suppress the superconductivity, and thus may be useful to reveal the role of spin fluctuations in the mechanism for the superconductivity. In unhydrated Na_xCoO_2, it has been shown that applied fields of several Tesla affect the thermopower and magnetoresistance in samples with x=0.68-0.75. We can investigate how large fields affect the spin-density wave state, and whether a metamagnetic phase transition occurs. X-ray scattering experiments in high magnetic fields can probe field-induced changes in the charge and orbital correlations. For x=0.5, there is evidence that fields on the order of 40 Tesla can melt the CDW state[74]. Synchrotron x-ray diffraction would allow us to probe this more directly.

2.2.5 Heavy Fermion – non Fermi Liquid Materials

Interested Participants: Paul Canfield, Pengcheng Dai, Carsten Detlefs, Brian Maple, Thom Mason, James Rhyne

Brian Maple discussed correlated electron physics arising from hybridization of localized *f*-electrons and delocalized conduction-electron states in numerous systems. This is a vast area of active research where competing interactions and coupling between spin, charge, lattice degrees of freedom give rise to novel electronic ground states such magnetic and quadrupolar order, valence fluctuations, heavy fermion behavior, hybridization-gap semiconductivity (Kondo insulator behavior), non-Fermi liquid behavior and unconventional (p- or d-wave) superconductivity. A lot of these materials are near quantum criticality where their second order phase transitions can be suppressed to 0 K by tuning a control parameter such as the magnetic field. Some model systems are $CeIn_3$, $Ce(Rh_{1-x}Co_x)In_5$, $PrOs_4Sb_{12}$, UGe_2, $Sc_{1-x}U_xPd_3$, and $URu_{2-x}Re_xSi_2$.

In particular, $PrOs_4Sb_{12}$ is the 1st Pr-based heavy-fermion superconductor (T_c = 1.85 K; all others based on Ce or U). In this material the formation of heavy Fermi liquid and superconductivity may involve electric dipole, rather than magnetic dipole, fluctuations. In sufficiently high field an ordered phase (HFOP) appears which is identified as antiferroquadrupolar order. In general, x-ray scattering is ideal for the study of multipolar order in 4*f* and 5*f* electron systems. This is because large resonant enhancements (4*f* L-edges and 5*f* M-edges)
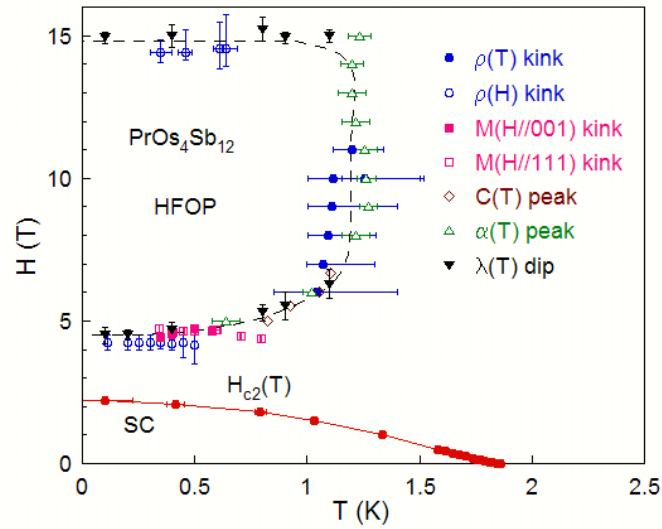
Figure 16 Multiple field and temperature dependent phases in PrOs$_4$Sb$_{12}$

and polarization sensitive cross sections provide a direct coupling to such order parameters. From zero field studies of materials such as NpO$_2$, presented by C. Detlefs (ESRF), a novel octupolar ordering was discovered. Such phenomena may be related to the puzzling phases in URu$_2$Si$_2$ as well. This material, as shown in Figure 17, has multiple phases as a function of temperature and magnetic field[75].
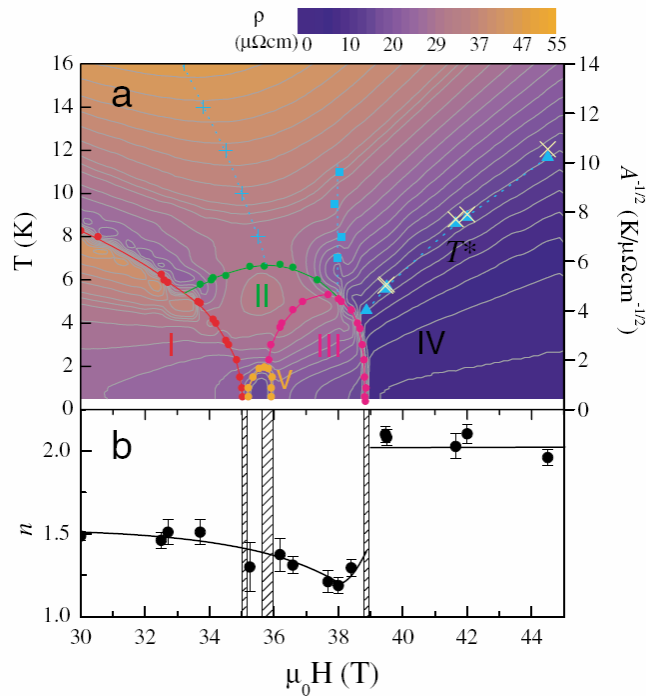
Figure 17 High field phase diagram for URu$_2$Si$_2$ (ref 75)

These phases have been isolated using the bulk probes of magnetization and electrical conductivity. However to identify the magnetic structure of these phases neutron diffraction is required. Low field work (Figure 18) has illuminated some of the features of Phase I ("Hidden Order Phase").[76] These features are summarized by a reduction of the (111) reflection as a function of magnetic field as shown in Figure 18
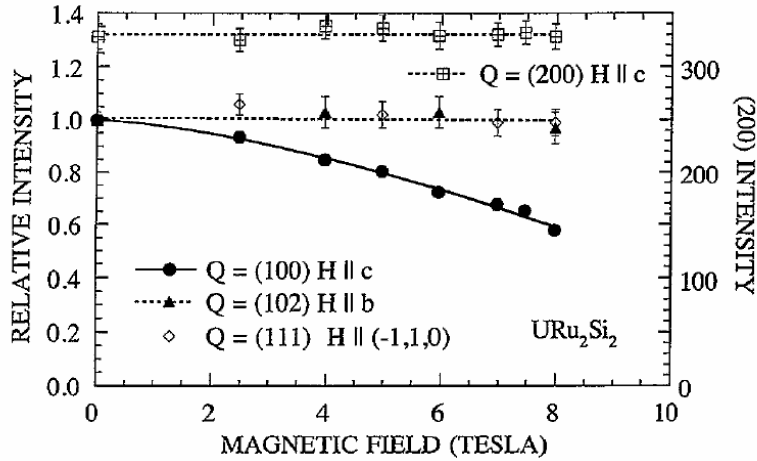
Figure 18 Relative intensity of several Bragg Reflections in URu$_2$Si$_2$ (ref. 76)

However note that the (111) reflection is far from disappearing. Therefore the current magnetic field capablilities at neutron sources can not probe beyond phase I. The excitation spectrum in URu$_2$Si$_2$ also reveals aspects of the nature of the material. Results shown in Figure 19 from Phase I reveal a singlet-triplet like gap[76].
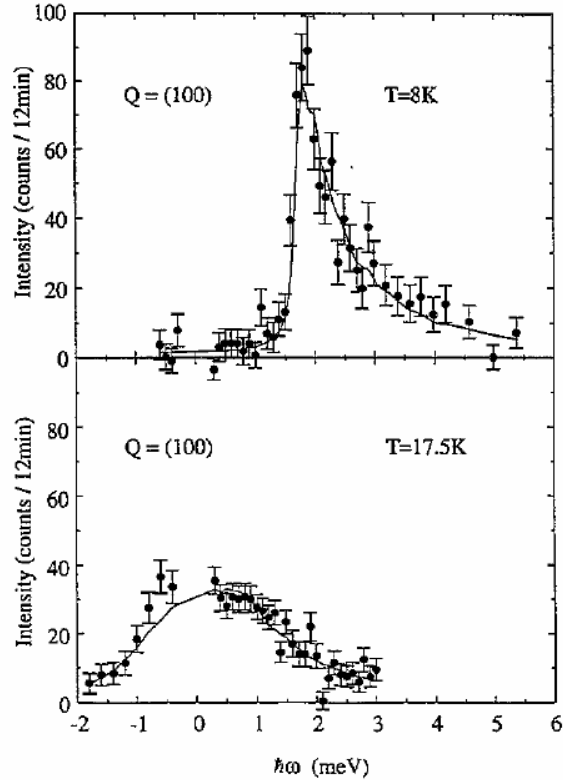
Figure 19 Excitations observed in URu_2Si_2 (ref. 76)

The lowest important energy scale in this system is this gap. The size of this gap suggests a minimum field of 15 T where the properties of URu_2Si_2 may start to change. However the fact that phase transitions are first observed at 35 T by bulk probes, suggests that a larger energy scale is more important. Therefore neutron experiments coupled with fields at least as high as 15 T are required to probe farther into the multiple phases in the system and fields as high as 40 T are required to full sort out the properties of URu_2Si_2.

2.2.6 Metamagnetism

Interested Participants: Paul Canfield

The topic of metamagnetism was extensively covered by Paul C. Canfield. Some of the most interesting phenomena in solid state physics pertain to the "structural" changes brought about by the application of high magnetic fields. These include the transformations of flux-line lattices in recently discovered rare-earth borocarbide (RNi_2B_2C, R is a rare-earth element) superconductors, and metamagnetic phase transitions in a large number of rare-earth intermetallic compounds, such as RT_2X_2

(e.g. T=Ni,Co; X=Si,Ge) and $RAgSb_2$, in high magnetic fields. An intricate balance between the long-range indirect exchange interactions and crystal electric field effects in these materials results in a rich and anisotropic field-temperature phase diagrams. These diagrams reveal existence of numerous complicated low-temperature phases in external

31
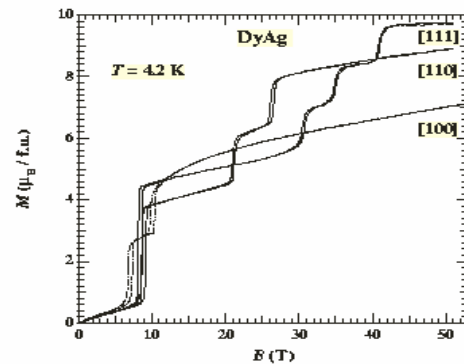
fields with varying range. CEF energy scales are of the order of room temperature (300 K) and for a moment of $10\mu_B$ (*e.g.* Dy and Ho) a vast number of such phases can be accessed in within 30 T. However, exceptions can easily be found; for example, in DyAg a simple cubic material with one magnetic ion per unit cell, all the metamagnetic phases appear above 10 T and require 30-50 T to access most of them. On the other hand in the uniaxial antiferromagnet $TbNi_2Ge_2$ compound a series of at least six distinct field-induced phases have been identified before the ferromagnetic ground state is reached below 10 T. High-resolution resonant x-ray scattering in zero field observed an IC-C magnetic phase transition into a complex magnetic structure which is described by a set of four propagation vectors. Neutron-diffraction studies in magnetic field revealed significant overlap of magnetic peaks and the metamagnetic phases remained unresolved. High-resolution magnetic x-ray scattering can shed clear insight in metamagnetic phases in such materials.

2.2.7 Orbital Ordering

Systems with open but fairly localized d- or f-shells, such as transition metal, rare earth, or actinide oxides, have been shown to exhibit a rich variety of ordering phenomena involving their charge, orbital, lattice, and spin degrees of freedom. The interplay between these degeneracies plays a critical role in determining the physical properties displayed by these compounds. By directly probing the ordered orbitals, resonant x-ray scattering provides a powerful tool for studies of this complex ordering.

NpO_2 provides a particularly intriguing example[77]. Upon cooling it exhibits a single-phase transition at T=27K. The exact nature of this phase transition, however, is still a subject of intense debate. Neutron scattering, susceptibility, and Mössbauer spectroscopy measurements suggest that this compound looses its magnetic moment entirely in the low temperature phase. The loss of a moment in this material, however, would be impossible, since in the absence of interaction breaking time-reversal symmetry, the ground state has to carry a magnetic moment regardless of crystalline environment. Recently, resonant x-ray diffraction studies have shown a long-range order of quadrupolar moments of the Np 5f orbitals.[1] While this alone does not explain the observed loss of the moment, a model where the primary order is octupolar, and the observed quadrupolar moment is an induced, second order effect would. Verification of this model, however, requires in-field measurements since this higher order orbital moment is not directly observable using conventional resonant x-rays scattering. In a large applied field, magnetic dipole moments should be induced on the Np sites. The symmetry of these moments is expected to follow the symmetry of the proposed primary octupolar moments and the secondary induced quadrupolar moments, therefore allowing for a direct measurement of the octupolar order parameter.

3 Structured Materials

3.1 Magnetic transitions at high fields in thin films

Interested Participants: Suzanne te Velthuis, Helmut Fritzsche, Mike Fitzsimmons, Frank Klose, Hal Lee, Christine Rehm

Understanding the behavior of magnetic thin films is of great interest for fundamental reasons and for their industrial applications. From the fundamental point of view, thin films offer the opportunity to study materials in reduced dimensionality, the influence of surface effects, or even more importantly the interaction between different materials, as can be probed by creating heterostructures. From the industrial applications point of view thin films in the form of magnetic spin valves - a heterostructure that utilizes both the exchange bias and exchange coupling phenomena - have and are continuing to significantly impact in the magnetic recording industry. Generally, high magnetic fields are needed to elucidate the magnetic structure of thin films and understand the physics of thin magnetic films wherever large magnetic anisotropies or large exchange interactions are involved. Because of the additional surface anisotropy present in thin films the magnetic anisotropies and the magnetic fields needed to get the sample magnetically saturated are in many cases orders of magnitude higher than in bulk samples.

3.1.1 Exchange bias

Exchange bias, which refers to the shift of the magnetization curve of a ferromagnet (FM) that is exchange coupled to an adjacent antiferromagnet (AFM), was first discovered by Meiklejohn and Bean[78] in 1956. The incorporation of exchange biased layers into spin valves, essential components of read heads in magnetic recording devices, has instigated an immense scientific interest in these systems for the last decades[79]. In most studies, exchange bias is probed by changing the applied magnetic field and thereby changing the state of the ferromagnet. Subsequently, the change in the ferromagnet is measured by for example, magnetometry, resistivity, magnetic imaging, or polarized neutron scattering, in order to try to understand the coupling at the interface between the two materials. However, many remaining questions within the field of exchange bias deal with the order within the antiferromagnet. Important issues are: the orientation of the antiferromagnetic spins relative to the ferromagnet, the number and location of uncompensated moments in the AFM, the relationship between these uncompensated spins and the AFM domain size, and other effects that influence this domain size.

While ferromagnetic (FM) materials can generally be well characterized (M(T,H,depth)) in moderate magnetic fields, it is a more challenging to learn about the antiferromagnetic spin ordering. For neutron experiments on AFM thin films the extremely small volume of material is the limiting factor. By growing multilayers of AFM layers, spaced by another type of layer, and creating sufficient bilayer repeats, one can increase the volume. Unfortunately, this cannot be done indefinitely, as sample quality deteriorates due to accumulating roughness. Despite this challenge, diffraction measurement have been

successfully performed to obtain the AFM spin orientation of CoO in Fe_3O_4/CoO multilayers[80], the spin density wave of Cr ref.(81), and even magnons in Dy/Y multilayers in as little as 10mg of material[82]. The antiferromagnetism can be influenced by a magnetic field, as illustrated in Figure 20, where the antiferromagnetic ordering in $Zn_{0.2}Fe_{0.8}F_2$ was studied relative to the field applied during cooling through the Néel transition[83]. This experiment showed that the AFM domain size increased with cooling field. While the field in this experiment was limited to 10 T, the result indicates that higher fields could possibly increase the domain size even further, forming an AFM single domain.
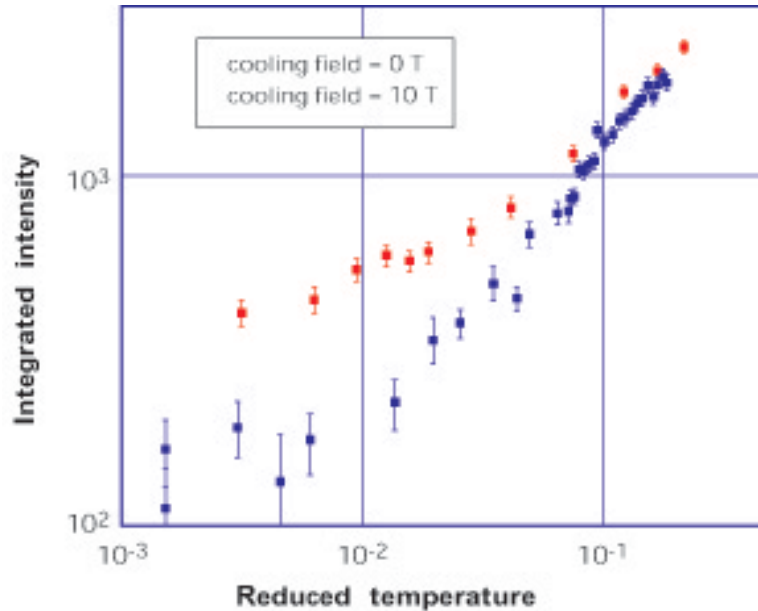
Figure 20 Integrated AFM Bragg peak intensity from single crystalline $Zn_{0.2}Fe_{0.8}F_2$ measured during increasing temperature after cooling with and with out an applied field [83]. The difference between the two curves indicates an increase of the AFM domain size with increasing cooling field.

Another approach to studying AFM behavior would be by inducing transitions to ferromagnetic or paramagnetic states, which would be easier to probe by polarized neutron reflectometry, which allows for the depth dependent ferromagnetic magnetization to be determined. The magnetic fields necessary to induce such transitions are inherently large, as they would compete with the magnetic exchange interactions within the AFM. In a study of polycrystalline Fe grown on single crystalline MnF_2, it was shown that there was a strong dependence of the exchange bias field (H_E) on the field applied during cooling through the Néel temperature of MnF_2 (Figure 21). A transition in H_E at high field (9 T) was correlated with the spin flop transition[84,85] in MnF_2, where the AF spins suddenly orient at 90 degrees with the applied field direction and above which, paramagnetic order occurs. While due to the moderate exchange field in MnF_2, the spin flop field is only 9T at 10K, in a similar antiferromagnet of equal interest, FeF_2, that field is 40T. Much could be learned about the exchange interaction between the FM/AFM layers either with neutron reflectometry or diffraction if fields sufficient to induce this transition (at least 40T) could be applied during the measurement.
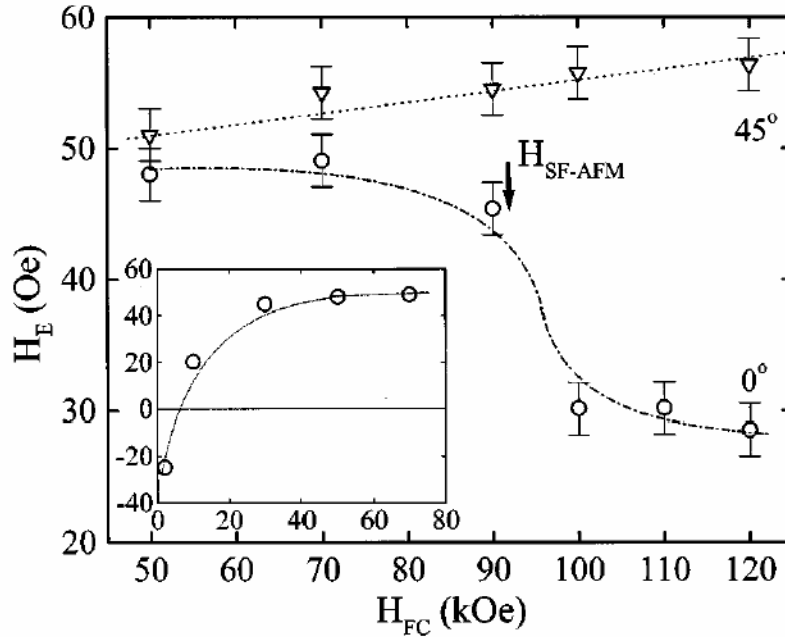
Figure 21 Dependence of the exchange bias field for Fe/MnF$_2$ as a function of cooling field from Ref. 84. The jump in H$_E$ at 90 kOe is due to the spin-flop transition of MnF$_2$.

3.1.2 Field induced transitions in complex oxide materials

Complex oxides, such as the perovskite colossal magnetoresistive manganites, are of great interest due to their wide range of interesting physical properties and complex phase diagrams which depending on doping and temperature. Additionally they can exhibit first order field-induced transitions, for example, from an antiferromagnetic charge-orbital ordered insulating state to a ferromagnetic metallic phase[86,87]. While these materials have primarily been investigated in bulk form, due to their potential applications in devices, interest is expanding to thin films. As thin films the influence of strain imposed by, for example, the type of substrate on the stability of various phases is important. Additionally the opportunity arises to create heterostructures, which allows the study of interface phenomena and proximity effects between mutually exclusive types of long-range order such as superconductivity and ferromagnetism. The study of these materials require high magnetic fields (>20 T), as the strain can increase the anisotropy and the magnetic field at which the relevant transitions take place[86,87], in combination with a high sensitivity to details of the magnetization within the films, such as can be provided by polarized neutron reflectometry.

3.1.3 High anisotropy films

The interest in high anisotropy materials, such as (DyFe$_2$/ErFe$_2$) multilayers, arises from the fact that the free energy is a sum of many competing terms, e.g. in this case, the bulk anisotropy favors the <100> directions for DyFe$_2$ but the <111> directions for ErFe$_2$ with a preferred parallel alignment of the Fe magnetization due to the Fe-Fe exchange interaction. Therefore, interesting magnetic structures may occur in these systems. The

intensity of the crystalline Bragg peaks is always composed of a nuclear and a magnetic contribution. So, to be able to separate the magnetic from the nuclear contribution to the diffracted intensity it is necessary to apply the magnetic field parallel and perpendicular to particular scattering vectors because the magnetic contribution is zero with the magnetization parallel to the scattering vector and maximum with the magnetization vector perpendicular to the scattering vector. For this type of experiment it is essential to have a **horizontal** magnetic field. However, the success of this method relies on the capability of pulling the magnetization parallel to the applied field. Because of the huge anisotropies present in these rare earth materials (e.g. larger than 50 T for bulk ErFe2 at 4K) in a previous study[88] it was not possible to pull the magnetization in a field of 2.6 T completely along particular directions even at room temperature. Hence, in order to explore the magnetic structure in these rare earth systems properly, there is definitely a need of huge **horizontal** magnetic fields (as large as possible).
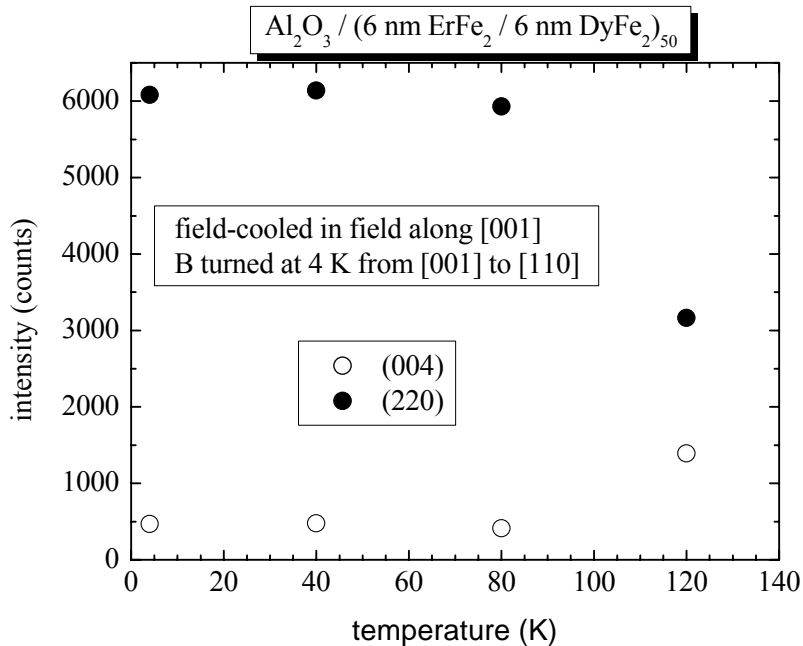
Figure 22 Intensity of the (220) and (004) Bragg peak as a function of temperature from Ref 88. The sample has been field-cooled in a field of 2.6 T along the [001] direction and at 4 K the field direction has been switched along [110].

As can be clearly seen from Figure 22 there is no change in magnetic intensity from 4 K up to 80 K because the magnetic anistropies are too large to be overcome by a field of 2.6 T. A temperature increase to 120 K is needed in order to start a rotation of the magnetization towards the field direction. This can be concluded from the fact that the intensity of the (220) peak with its scattering vector parallel to the field direction decreases.

4 In-field material processing

4.1 Exploring Ultrahigh Magnetic Field Processing of Materials for Developing Customized Microstructures and Enhanced Performance

Interested participant: Gerry Ludtka, Frank Klose
Other Interested Researchers: Roger Kisner, Gail. Mackiewicz-Ludtka, John Wilgen,
Roger Jaramillo, Don Nicholson, Sudarsanam Babu (Oak Ridge National Laboratory),
Peter Kalu (Florida A&M University- Florida StateUniversity/ National High Magnetic
Field Laboratory), and R. D. England(Cummins, Inc.)

4.1.1 Introduction

A review of any of the excellent NHMFL Annual Reports and subsequent refereed journal publications from those research endeavors rapidly highlights the significant scientific and technological breakthroughs achievable across many research disciplines through ultrahigh magnetic field experiments. Major research enhancing developments are occurring simultaneously around the world that undoubtedly will accelerate discovery of the next generation of materials. An example of these that is underway at ORNL is the completion of the SNS. The SNS will provide the most intense (1.4 MW) pulsed neutron beams in the world for scientific research and industrial development.

Research on ferrous alloys[89,90,91,92,93,94,95] has clearly shown experimentally and through ab-initio modeling endeavors that phase stability can be dramatically altered through the application of an ultrahigh magnetic field. This ability to significantly influence the phase stability of parent and product phases provides the ability to tailor and precisely control microstructure for a specific application. Therefore, the simultaneous use of a strong magnetic field and thermal processing promises to be a very robust mechanism to develop uniform and reproducible microstructures in ferrous alloys.

An applied magnetic field has a direct thermodynamic influence on the chemical potential (Gibbs free energy) of the various phases in a material. This is clearly shown in the following equation for calculating the Gibbs free energy change for iron for the ferrite, α, to austenite, γ, phase transformation in a Fe-C binary alloy in the presence of an applied magnetic field:

$$\Delta G_{Fe}^{\gamma \to \alpha} = RT\left[\ln a_{Fe}^{\gamma} - \ln a_{Fe}^{\alpha}\right] + \int_{0}^{H} \left(M_{Fe}^{\gamma} - M_{Fe}^{\gamma}\right)dH, \qquad (1)$$

where *M* and *H* are defined as the magnetization and the magnetic intensity, respectively. This effect will be manifested in the Fe-C binary equilibrium phase diagram as shifts in the transformation temperatures of the various phases as well as changes in the solubility limits (solvus lines) of the various phases. The main requirement for this proposed magnetic process to be effective is that the parent and product phases need to exhibit different magnetization responses to the applied magnetic field. This property clearly exists for ferrous alloys.

4.1.2 Current Magnetic Processing Research Limitations

The significant ramifications of magnetic field processing for developing the next generation of materials with dramatically enhanced performance are shown in the following figures. Experimental and modeling results from continuous cooling experiments (nonequilibrium conditions) indicate that the pseudobinary equilibrium phase diagram for the SAE 1045 alloy steel is significantly shifted by the presence of a 30 T magnetic field as shown in ThermoCalc predictions depicted in Figure 23. Transformation temperatures, phase solubility limits, and phase volume fractions are all affected by magnetic field processing. This shift is supported by microstructural evidence as indicated in Figure 24 where the volume fraction of the BCC (body-centered cubic) ferrite phase is increased from 40% to 65% upon cooling in a 30 T magnetic field. This change in phase fraction can not be achieved by any other means and therefore supports the thermodynamic effect of magnetic fields on materials that change magnetic character (ferromagnetic to paramagnetic) upon cooling.
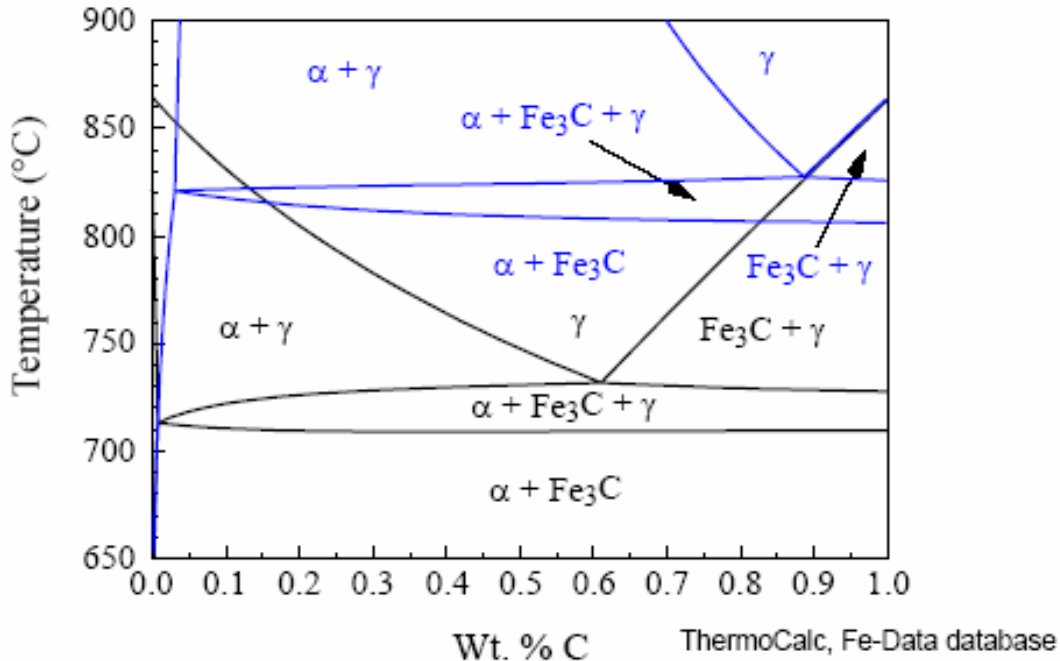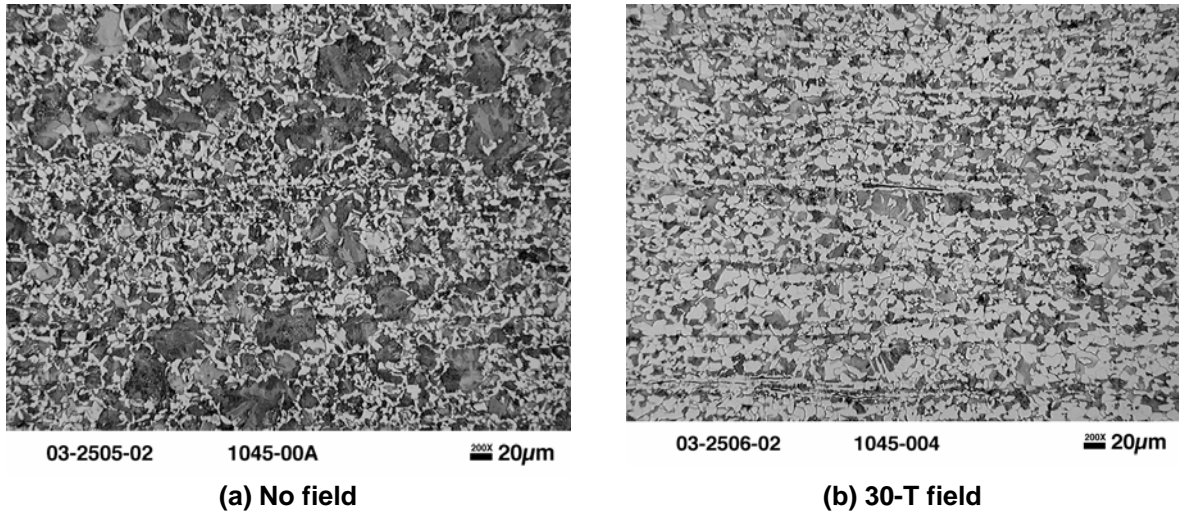

Figure 23. Prediction of the pseudobinary phase diagram for an SAE 1045 steel for conventional equilibrium (black lines) and magnetically enhanced equilibrium (blue lines) based on estimated Gibbs Free Energy contributions from magnetic fields obtained from continuous cooling experiments under an applied 30 T magnetic field.

(a) No field   (b) 30-T field

Figure 24 Microstructure for SAE 1045 steel specimens cooled at 10°C/s: (a) 40% ferrite (light phase) formed without an applied magnetic field, and (b) 65% ferrite formed with an applied 30-T field (light micrograph).

Similarly, the metastable and equilibrium phase transformations that occur upon rapid cooling are influenced by magnetic fields. Materials scientists represent this behavior in Continuous Cooling Transformation (CCT) Diagrams that help summarize microstructural evolution during thermal processing behavior, such as heat treatment, in components that will experience different cooling rates at different depths within the part. Part of the CCT curve for the SAE 52100 steel is presented in Figure 25 where the influence of magnetic fields is shown to move the initial transformation start line (dotted black line) up to higher temperatures and to shorter times (blue line). This behavior is a function of the magnetic field strength as indicated in Figure 26 for the SAE 1045 steel where different magnetic field strengths are applied to different samples cooled at the same cooling rate. As the field strength is increased the transformation temperature as indicated by the onset of recalescence heating (exothermic enthalpy of transformation) is higher and starts at earlier times. Current microstructure analyses research methods which are conducted after the magnetic processing experiment haven't facilitated decoupling nucleation from growth effects to determine which (or both) is dominating the enhanced phase transformation events. This is especially critical in understanding the implications of the following results on a high strength, "Super Bainite" alloy that holds the promise for enabling bulk nanocrystalline microstructures to be achieved readily through magnetic field processing.
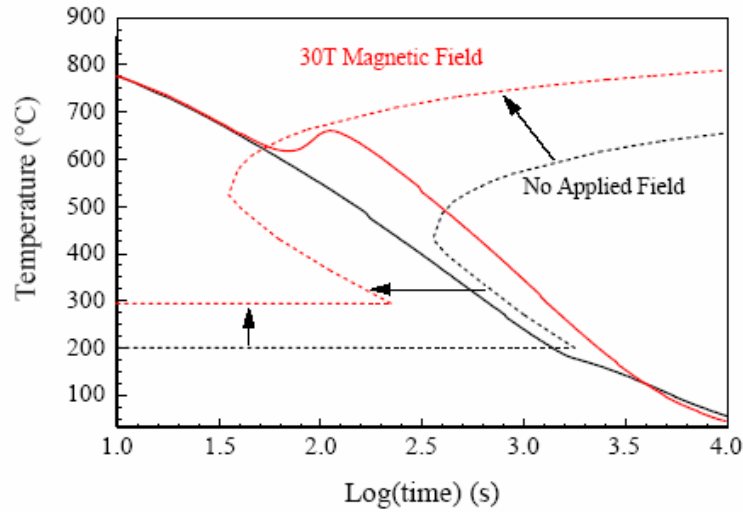
Figure 25 Application of a 30-T magnetic field during continuous cooling moves the transformation start line in the continuous cooling transformation (CCT) curve for the 52100 steel upward to higher temperatures and to the left to shorter times (dotted red line) as compared with the conventional behavior (dotted black line) for this alloy. The solid lines are the cooling paths for the two test specimens with identical initial cooling rates.
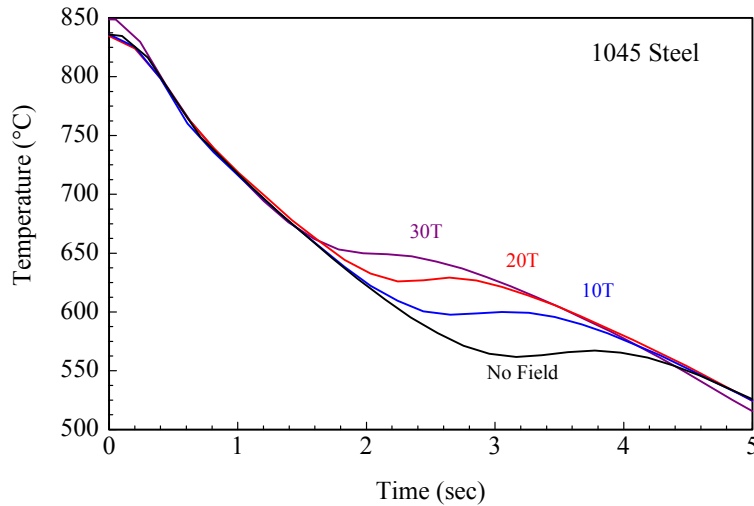
Figure 26 Continuous cooling path information for the SAE 1045 low-carbon steel alloy for different magnetic field strengths for the same initial cooling rate.

The results of the microstructural examination of the super Bainite material indicated in Figure 27 demonstrate that 50 nm spacing pearlitic microstructures are achieved in bulk samples through magnetic exposure during cooling. Although not shown here, hardness measurements of this microstructure were determined to be almost double the value achieved in conventionally processed pearlite. Therefore nanocrystalline feature microstructures with dramatically enhanced performance appear viable through magnetic processing.
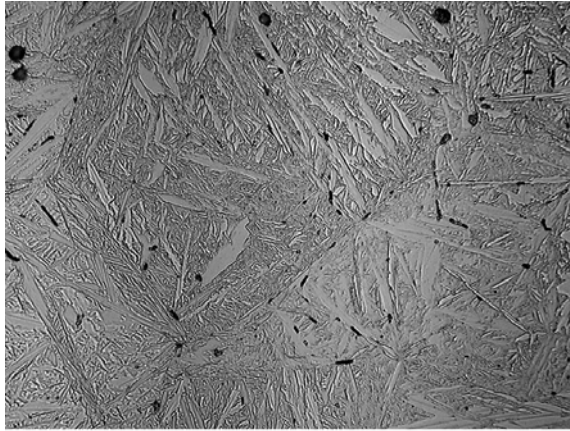
04-0100-03   SP11C-1 NFSC   500X 10μm

(a)
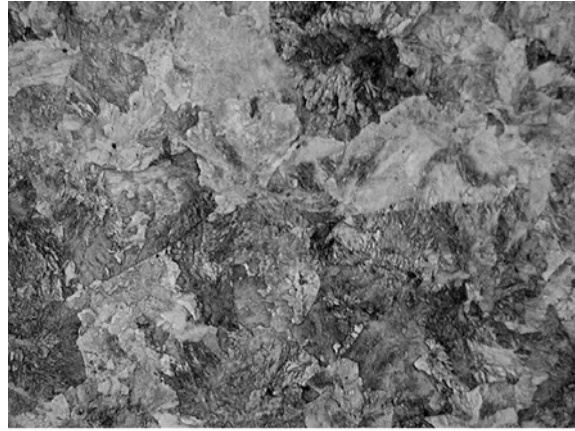
04-0101-03   SP11C-1 30TSC   500X 10μm

(b)
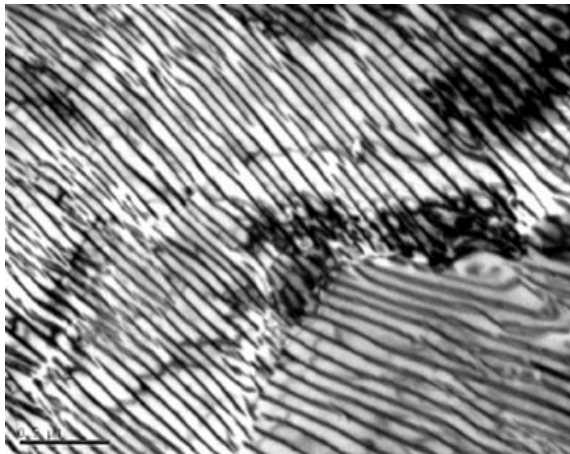
(c)

Figure 27 Microstructures of the high-strength bainitic steel specimens formed at a cooling rate of 1°C/s: (a) optical micrograph of the "no-field" experiment showing the fully martensitic microstructure; (b) optical micrograph of the 30-T experiment showing a microstructure typical of cellular decomposition and no martensite; (c) bright field transmission electron micrograph of the 30-T specimen resolving the very fine 50 nm spacing pearlite microstructure.

The final example will be for isothermally processed Fe-15a/oNi where conventional x-ray measurements (results shown as red bands in Figure 28) on specimens examined after their processing with and without a magnetic field show that enhanced substitutional alloying element solubility occurs for both the FCC (γ) and BCC (α) phases as shown in Figure 28. Ab-initio Local Spin Density calculations that predict the magnetic moment alignment with and without an applied magnetic field (Figure 29) provide the magnetic free energy contribution that yields the blue bands shown in Figure 28. Noticeably there is slight discrepancy between measured and predicted values that may reflect the fact that the x-ray measurements were conducted at ambient temperature and are not of the microstructure as it existed at temperature under the applied field. Therefore, the LSD model may be accurate in predicting the high field effects but this conclusion can not be unequivocally made since there exists this disagreement with the available experimental data.
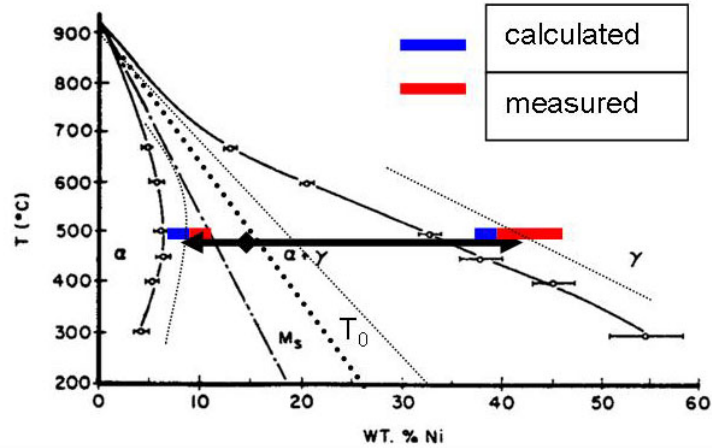
Figure 28 LSD modeling predictions of the shift in phase boundaries for the Fe-rich side of the Fe-Ni phase diagram under the imposition of a 29-T magnetic field. The dotted black lines and red bands (x-ray data) indicate the new phase boundaries (solvus lines) exhibiting enhanced Ni solute solid solubility under the influence of the applied field. The blue bands are the LSD predictions at this temperature.
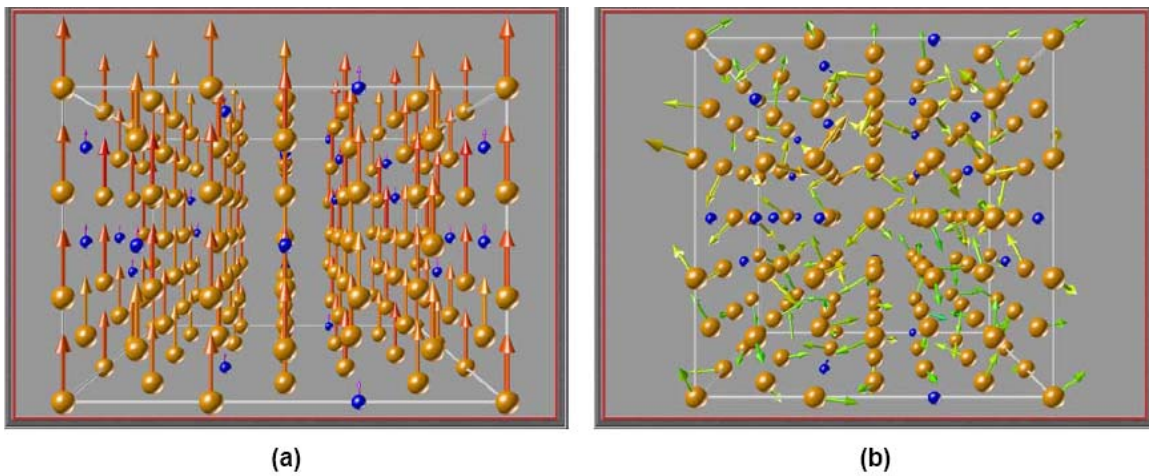
Figure 29 LSD predictions of the magnetic moment alignment of (a) the ferromagnetic α phase of Fe-15Ni and (b) the paramagnetic γ phase in Fe-15Ni. Gold spheres indicate iron atoms, and blue spheres indicate nickel.

Consistent throughout the research results presented above is the fact that all microstructural analyses and modeling validation were conducted on samples *after* the magnetic processing experiments were concluded. Therefore the influence of magnetic fields on phase equilibria existing at elevated temperature isothermal experiments was characterized on ambient temperature specimens without a magnetic field superimposed. There exists the definite possibility that some phase equilibria shifting occurred in these samples while cooling to ambient temperature even for those samples still under the influence of a magnetic field. This potential discrepancy can be significant when assessing the validity of fundamental modeling predictions which is critical to facilitate accurately predicting magnetically enhanced phase diagrams to drive future experiments and materials development efforts via magnetic processing. This line of reasoning can be carried through for all of the examples given here.

Of equal importance in understanding the influence of magnetic field processing on microstructure evolution and properties is the ability to deconvolute the impact of magnetic fields on nucleation versus growth phenomenon which influence phase transformation kinetics and morphology. Accurate microstructure evolution models will enable tailoring customized microstructures to achieve maximum performance enhancement which will yield bulk nanocrystalline alloys and superior strength alloys. Although not presented in this paper, magnetic fields have been shown to significantly influence the crystallization behavior of bulk amorphous materials which can lead to a new class of alloys. Critical to maximizing the potential of research in this area is the ability to monitor the onset and kinetics of embryonic crystal formation.

4.1.3 Justification and recommendations for probing matter using neutrons and X-rays under high magnetic fields

Establishing an ultrahigh field hybrid magnet system at the SNS will link the fundamental analytical capabilities inherent in neutron science to address these various in-situ, time-resolved characterization needs of magnetic processing research. This next generation neutron source facility will have increased incident neutron flux and increased detector coverage which will enable rapid data acquisition with high resolution.

Neutron diffraction spectra of magnetic materials contain 3 different contributions that provide significant information about the material. These are:

- Elastic neutron scattering that is due to both Bragg diffraction (periodicity of the lattice) and the neutron cross section of the nucleus (varies irregularly with atomic number and therefore can distinguish adjacent elements in the periodic table)

- Magnetic scattering due to the magnetic ordering and magnetic scattering cross section of the material

- Inelastic neutron scattering that results in the creation or annihilation of a magnon (spin wave excitation)

Therefore, neutron scattering studies will enable time-resolved, high temperature, bulk (rather than surface) crystal structure characterization (sensitive to light elements such as O, N, C, H), the investigation of nucleation and growth of secondary phases, measurements at the nano- and meso-scale (small-angle neutron scattering), the determination of magnetic moments (for fundamental modeling validation) and magnetic ordering, isotopic resolution, non-destructive residual stress mapping, and transparency to ancillary equipment. The one limitation relative to neutron scattering measurements is the requirement of relatively large sample volumes.

Implied in incorporating a hybrid magnet into the instrument suites at both the SNS and APS is the need for establishing various inherent capabilities during the design stage of the hybrid magnet so as to provide an analyses system rather than just a source of magnetic field strength. This concept is schematically depicted in Figure 30. To augment neutron or x-ray data, a high magnetic field system should incorporate various complimentary capabilities for non-contact, line-of-sight measurements of temperature (e.g., optical pyrometer or spectrometer) and dilation (optical dilatometer) as well as a closed-loop system for accurate control of heating and cooling the specimen to achieve

any desired thermal transient cycle. Incorporation of a digital video camera to monitor the sample during the experiments would also be beneficial.

Our research results and discussion presented here clearly show the significant science that can be accomplished using ultrahigh magnetic fields and support the need to establish robust ultrahigh magnetic field hybrid systems at the Advanced Photon Source and Spallation Neutron Source as "virtual" NHMFL User Facilities to facilitate advanced, time-resolved characterization research using x-ray and neutron techniques. These new research resources in conjunction with conventional analytical methods would facilitate developing the fundamental science necessary to achieve future major breakthroughs in research on magnetic field effects for a broad spectrum of materials beyond the systems discussed in this presentation.
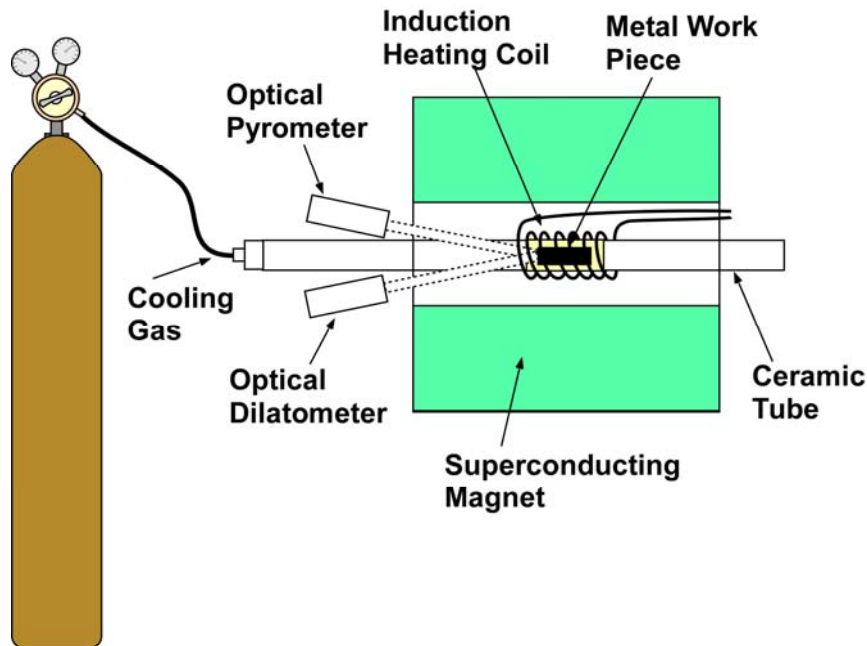
Figure 30 To augment neutron or x-ray data, a high magnetic field system should incorporate various complimentary capabilities for non-contact, line-of-sight measurements of temperature (optical pyrometer or spectrometer) and dilation (optical dilatometer) as well as a closed-loop system for accurate control of heating and cooling the specimen to achieve any desired thermal transient cycle.

5 Other science possibilities

From discussions at the workshop, other types of science were identified that could utilize high magnetic fields and neutrons.

5.1 Flux lattice measurements

Other Interested Researchers: Mohana Yethiraj (Oak Ridge National Laboratory), Morten Eskildsen (University of Notre Dame)

When a type II superconductor is placed in a magnetic field, it is threaded by swirling whirlpools of electric current known as vortices or flux-lines.   The vortices are

fascinating massive entities, that can serve as an unique probe of the host superconductor. Small-angle neutron scattering (SANS) can provide detailed information about the inhomogeneous internal field distribution. At low fields SANS is complemented by imaging and muon spin relaxation techniques while at fields above 5 T neutrons are the only viable structural probe. FLL diffraction experiments are typically carried out on SANS instruments in horizontal fields up to 8 Tesla. Such experiments allow determination of the FLL symmetry and domain structure, and the vortex form factor, which reflects the unit cell field distribution. Higher fields lead to smaller distances between the flux lines and access to the magnetic field distribution closer to the core of the flux line. The scale for the interesting field range is set by the upper critical field, H_{C2}, which for high T_C superconductors is in excess of 100 Tesla.

A commonly observed phenomena in both low- and high-T_c materials is a transition from a hexagonal FLL at low fields to square symmetry at higher fields[96,97,98,99,100,101,102]. Studies of this FLL transition have improved our understanding of the details of the superconducting transition in systems such as the borocarbides, A15 materials (V_3Si, Nb_3Sn), and MgB_2. While the transition in conventional superconductors is ascribed to non-local effects[103,104], the driving mechanism in e.g. YBCO is currently under debate. In addition to non-locality, the d-wave nature of the Cooper pairs in the high-Tc materials is also predicted to lead to a square FLL[105]. Extending the measurements to higher fields increases the accessible fraction of HT-phase space, which in turn greatly improves prospect for determining the importance of these two mechanisms. Even in some conventional superconductors, the available field range severely limits the fraction of the phase diagram that can be probed. The A15 systems for example have an H_{c2} of about 20 Tesla and MgB_2 has an in-plane H_{c2} of 16 Tesla that increases to over 50 Tesla with doping. For the latter material, which has considerable potential for applications, FLL neutron scattering is turning out to be critical for understanding the contributions of different parts of the Fermi surface to superconductivity.[106,107]

5.2 Hydrogen Related Structure and Function

Other Interested Researchers: John Root

Although magnetism studies on promising hydrogen storage materials are less interesting simply because most of them are non-magnetic, very high magnetic fields have great potential for directly studying the behavior (location, binding, local environment etc.) of the absorbed hydrogen atoms. New experimental techniques are feasible, including the following:

i) With a 35 T magnet one can align protons in an external field. Using a polarized incident neutron beam, the nuclear spin-incoherent cross section, which usually creates a huge background signal, is eliminated and structural work on metal hydrides can be done much more precisely without the need of H-D exchange.

ii) Fuel cells should work with H rather than with D. In-situ and real time neutron radiography on the diffusion of polarized hydrogen through fuel cells can be performed for controlling homogeneity and efficiency of fuel cells.

iii) Using a high magnetic field, experiments can be done similar to MRI in medical applications. First the protons are aligned in the field. Then with an rf-coil the protons are turned by 90° or 180°, which relax back to the original orientation within some

longitudinal and transverse relaxation time. Certainly, this experiment can also be done and has been done by NMR methods on metal hydrides. Using neutron scattering at the same time bears some additional charm. As the cross-section depends on the total neutron-proton angular momentum, neutron imaging can be performed of the protons and contrast can be achieved by the virtue of different relaxation times. In case of fuel cells, for instance, defects causing different relaxation times could be imaged. Different relaxation times are also caused by magnetic impurities or chemical reactions. Therefore, with the combination of neutron radiography and proton relaxation the precise reaction zone of the hydrogen / oxygen reaction at the surface of a fuel cell can be imaged.

Hydrogen is considered as an attractive candidate for energy storage and management in vehicles because its reaction product is water, and does not add to the planetary burden of greenhouse gases. However, on attempting to introduce a hydrogen economy, it is well understood that "Current technology is promising but not competitive. More emphasis is needed on solving fundamental science problems."[108] Storage of hydrogen in sufficient density for automotive applications is a key challenge. Neutron scattering from materials that are subjected to a wide range of temperatures, pressures, magnetic fields and other conditions is the most effective method to explore the underlying molecular structures and processes in bulk materials. The high, isotope-dependent, sensitivity of neutron scattering to hydrogen is a particular benefit to investigations of hydrogen absorbed into crystalline lattices, or carbon-based adsorption materials, which are candidates for the safe and efficient storage of hydrogen. Many alloys from current metal hydride systems are based around alloys of transition metal ions or rare earths, elements to which neutrons are uniquely sensitive probes for crystallographic site ordering. At the same time, these atoms respond to magnetic fields, so the combination of neutron scattering from specimens subjected to high magnetic fields opens up the widest possible vista to explore and discover the materials that may accelerate progress towards meeting the expectations of consumers in a hydrogen economy: volume stored vs. mass of container, speed of storage and extraction, longevity of the storage material vs. cycling and so on.

5.3 Magnetic resonance signals detected by neutrons

Magnetic resonance techniques us a magnetic field to split the spin states of a system and then use electromagnetic radiation to excite a resonance between these two states. Typically two systems have been considered: unpaired electrons in molecules and the nuclear spin states of nuclei. Neutrons incident on the system can also induce transitions between the spin states by an associated change of energy.

The utilization of neutrons to probe resonant systems has a couple of general advantages. First neutrons interact with the spins through a different coupling mechanism than electromagnetic radiation. Therefore some transitions that are forbidden by the electromagnetic interaction selection rules can be observed with neutrons. Second systems with large numbers of conduction electrons have a limited penetration depth. Neutrons do not have this restriction and thus the full sample can be probed and sample shapes do not have to be manipulated to ensure resonance detection. Sections 5.3.1 and 0 discuss the potential application of neutrons to the electronic spin case and the nuclear spin case respectively.

5.3.1 Electron Paramagnetic Resonance

Interested Participants: Garrett Granroth
Other Interested Researchers: Al Beth (Vanderbilt University)

As a magnetic field is applied to an unpaired electron the splitting of the energy levels goes as 0.116 meV/T. Large enough fields to observe this splitting has only recently become available with the advent of magnets that can achive10 T and thus the field splitting would be 1.16 meV. However for sufficient g factor resolution, fields greater than 30 T and resolutions on the 1 μeV are required. Therefore this technique required cold incident neutrons and near backscattering crystal analyzers.   Neutron probed Electron Paramagnetic Resonance will be particularly useful for examining biological systems as is described in the following paragraph.

Electron Paramagnetic Resonance (EPR) spectroscopy is utilized extensively to characterize the molecular environment of unpaired electrons in samples ranging from biomaterials, to isolated biomolecules, to free radicals in intact tissues and organisms. The vast majority of EPR experiments are conducted at X-band (8-9 GHz) microwave frequencies where the unpaired electron resonates in a static external field on the order of 0.3 Tesla. In the past decade, there has been a major thrust to obtain EPR data on biological samples at higher fields/frequencies in order to improve spectral resolution due to the anisotropic nature of the g-tensor, to improve sensitivity to various dynamic processes, and or in systems with large zero-field splittings[109,110,111]. Though such measurements are rich in information, they are extremely challenging due to the necessity of obtaining data in an aqueous environment where microwave absorption is a severe complication. Though many advances in resonator design have occurred, it remains an extreme challenge to get EPR data on biomolecules even at frequencies of 250 GHz where resonances occur at approximately 9 Tesla. In practice, one is forced to work with extremely small (on the order of 10-100 nL) aqueous samples at microwave frequencies in the 95 to 250 GHz range. The use of neutrons as an excitation source should overcome many of the current sample size limitations and permit observation of electron resonances at very high magnetic fields where spectral resolution is enhanced. This new class of neutron experiments holds the potential to be an important complement to classical resonance experiments for a wide range of macroscopic biological samples. Two areas of application for these new measurements would be in characterizing the paramagnetic metal centers in metalloenzymes in solution where very large zero-field splittings often preclude observation of resonances at low fields/frequencies and in quantitating the partitioning of spin-labeled molecules between different phases such as between the cell membrane and the extracellular space where the g-tensors are subtly different.

5.3.2 Nuclear Magnetic Resonance

One interesting discussion that emerged during the talk of G. Aeppli is the possibility of using Neutrons to detect nuclear magnetic resonance (NMR) signals.   The NMR technique uses a magnetic field to split the degenerate spin states of magnetic nuclei and then uses a probe with a frequency equal to that splitting to excite a resonance between these states.   The details of the splitting reveal details of the environment around the nuclei. The magnitude of the nuclear gyromagnetic ratio means that for typical magnets

the required frequency is in the MHz range. Therefore the traditional probe for the resonance is radio frequency (RF) electro magnetic radiation. Unfortunately the characteristic frequency of neutrons is on the order of THz so the splitting provided by the current state of the art neutron magnets will not allow resolution of the signal with neutrons. However if a field of 40T is available the splitting in frequency is now ~ 2GHz. Then with ~ 0.120THz incident neutrons, a spectrometer with 1% resolution would resolve these resonances. Finer resolution would be needed to see the detailed structure of the resonance. The numbers mentioned above assume spin ½ nuclei. If nuclei with a larger magnetic moment were to be studied, a 5 % spectrometer could resolve these resonances, but a very fine resolution instrument would still be needed to study the structures in the resonances. Alternatively a larger magnetic field would relieve the fine resolution requirements on the neutron instrument

6 Facility requirements

The groups that presented the science cases described above also provided the necessary instrument parameters to perform the described science. The requirements for the magnet are described in section 6.1. The requirements for a neutron instrument are summarized in section 6.4.1 followed by ideas for an instrument at the SNS in 6.4.2

6.1 Magnet requirements

	Molecular Magnets	Quantum magnetism	Systems with conduction electrons	Thin Films	Material Processing	Magnetic Resonance	Flux lattices
Max sample size		1 mm^3 to 10cm^3	10cm^3	6cm^2 by 3mm thick	10cm^3	10cm^3	10cm^3
Conditions							
T range	0.065-300K	0.05-300 K	1-300 K	4-400 K	0-1000° C	0.05-300 K	0.05-300 K
Orientation capabilities (how many axes?)	Powder not relevant	1 at 360° two supporting at 10°	3 axes			1 at 360° two supporting at 10°	1 at 360° two supporting at 10°
Polarization analysis?	no	yes	yes	yes	no	no	yes
Time dependent effects?	no	No	no	No	yes	no	no
Other?		Rapid equilibration and high accuracy (0.1%)			Other non contact probes		
Field							
Magnitude	<100T	> 35 T	> 40T	> 40 T	>30T	>35T	>40T
Direction relative to incident beam	not relevent	Horizontal or vertical	Horizontal and vertical	Horizontal and vertical	No preference	No preference	Horizontal
Split coil vs solenoid?	No preference	Largest possible solid angle	No preference	Both	No preference	No preference	
Access angles							
Split coil	As large as possible	As large as possible	As large as possible	As large as possible	As large as possible	As large as possible	As large as possible
Solenoid	As large as possible	As large as possible	As large as possible	As large as possible	As large as possible	As large as possible	As large as possible
Sample/sample environment size	5cm^3	Up to 10cm^3 sample. Effectively neutron shielded sample environment.	Up to 10cm^3 sample.		Up to 10cm^3 sample.	Up to 10cm^3 sample.	Up to 10cm^3 sample.

Table 1 Magnet requirements for a High field neutron Beamline

6.2 Preliminary Magnet Concepts

The National High Magnetic Field Laboratory magnet design staff presented two concepts for producing fields up to ~ 40 T for scattering geometries. These two concepts fit well with the magnet requirements in Table 1 for neutron instruments. One of these concepts is a "conical" configuration with a large scattering cone, the other is a "split" configuration with regular spaced openings to allow the neutrons in and out. Both configurations utilize the series-connected hybrid technology that is under development at the NHMFL to produce the maximum field with 10-12MW of power.

Figure 31 shows the basic concepts of a conical hybrid with a horizontal bore (and field), a large-bore superconducting coil and a conical-bore resistive coil. In this concept, the superconducting outsert coil is intended to be the same as the one being designed for use at the NHMFL's powered magnet facility[112]. The resistive coil and housing, as well as the cryostat would be significantly different. Conical magnets could also be built using entirely resistive technology. Figure 32 provides preliminary values of the central field that might be attained with such conical magnets either resistive or hybrid for various conical half-angles and power levels
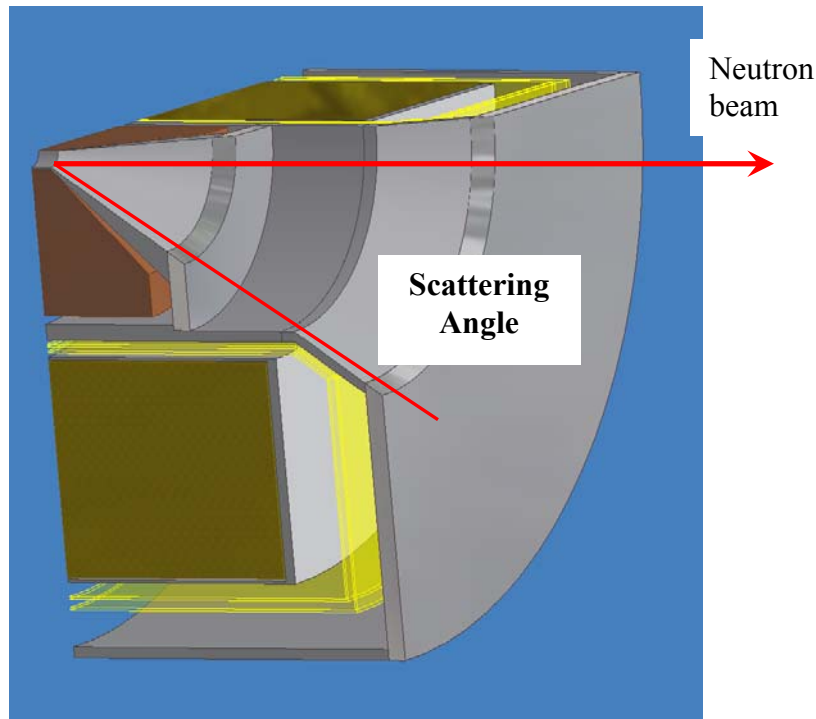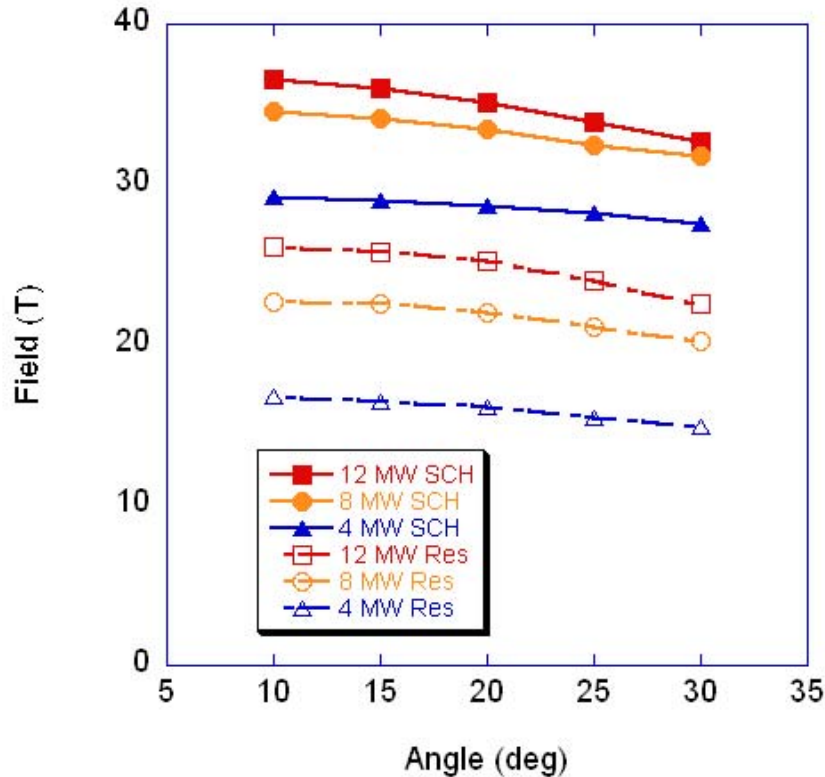

Figure 31 Conceptual layout of conical series-connected hybrid magnet.

Figure 32 Preliminary attainable field for conical powered magnets 40-mm bore and 20-mm samples with various power levels and conical half-angles.

We see that for fixed power, the Hybrid magnet provides approximately 15 T more field than does the resistive magnet. For magnets of the same field, the hybrid uses about 1/3 the power of the resistive magnet. As both the capital and operating costs are dominated by the size of he power supplies and cooling water systems, it appears one should choose the hybrid magnet over the resistive one.

For the split configuration, the trade-offs are more difficult to quantify. Clearly the field decreases as the split increases. However the split can be characterized by both a sample-size and a vertical take-off angle. The NHMFL has been working on a split magnet for far-infrared scattering experiments as shown in Figure 33. This magnet will have a sample size of 5 mm and a vertical take-off angle of +/- 5.7 degrees[113].
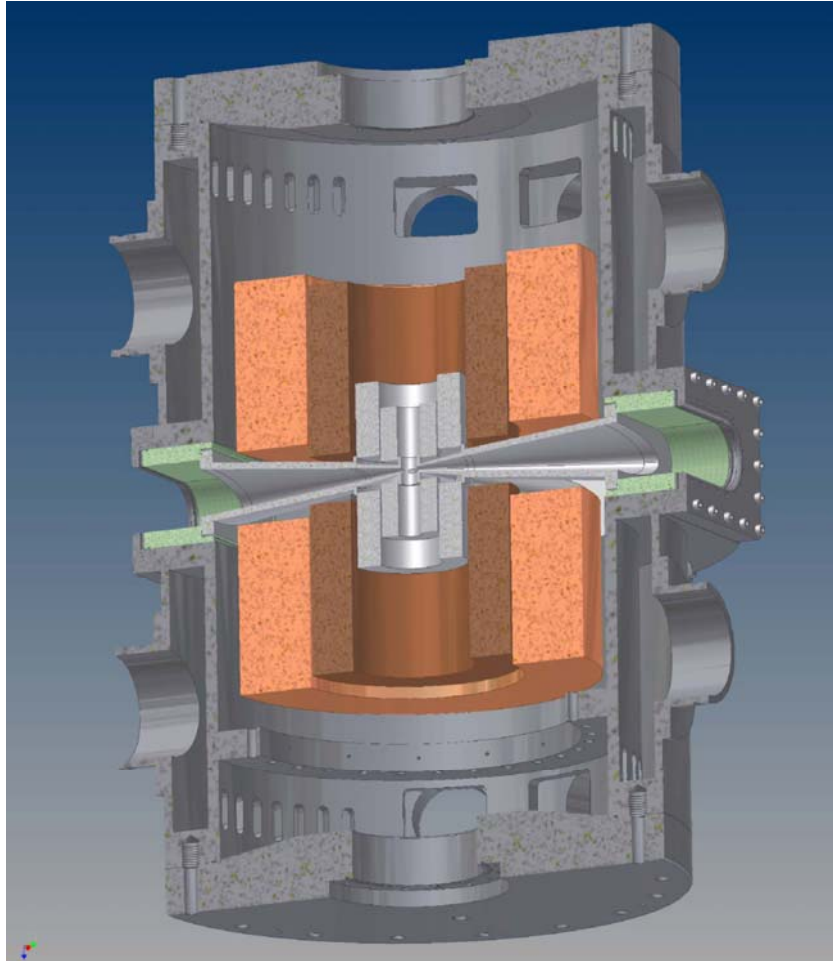
Figure 33 Preliminary section of 24-MW split resistive magnet at the NHMFL. There are four mid-plane ports, each of which subtends ~45 degrees. Hence, by rotating either the magnet or the beam, one can cover 360 degrees of scattering with two measurements.

Figure 34 provides preliminary attainable field values for split resistive magnets of various power levels and gap dimensions. Here the vertical take-off angle is zero. Again, hybrid magnets should attain similar fields with only ~1/3 the power of a resistive magnet.
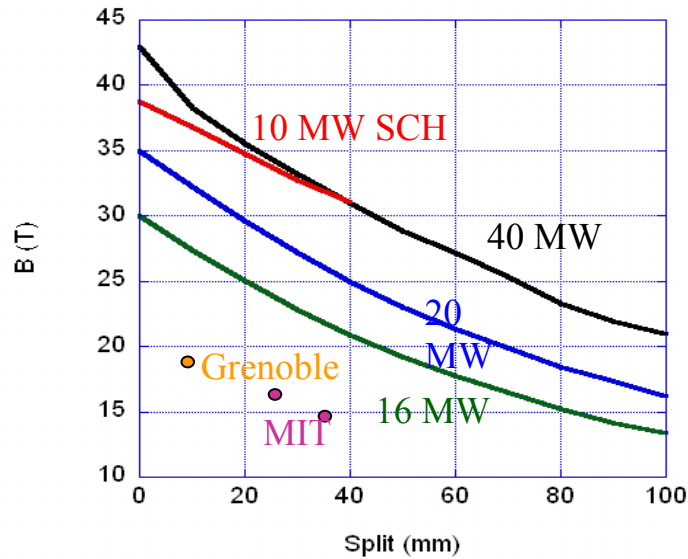
Figure 34 Change in field as a function of a coil split for the vertical field spit coil orientation. Several different powers are shown. The red curve shows the case for a 10 MW series connected hybrid

Concepts for magnets that fit well with the science case described in sections 2-5 are available and are ready for full design. The details of the exact magnet design will be worked out with the instrument personnel at the scattering facilities.

6.3 X-ray Instrument discussion

6.3.1 Current capabilities

Various magnets are available at synchrotron facilities worldwide. At the ESRF a 10T DC magnet is operational on an ID20 beamline. A 30 T pulsed-field magnet (on BM26 beamline) is available to carry out powder diffraction studies of structural transitions. With an appropriate data collection strategy this magnet is particularly useful in collecting powder patterns at a large number of fields up to 30 T in every pulse. A wealth of information on materials such as magnetocaloric materials, such as Gd-Ge-Si, which undergo field-induced crystallographic transitions can be obtained in a very short period of time. Such materials are potential candidates for future generation magnetic refrigerants. C. Nelson and Y. Ren discussed these materials.

Current capabilities for diffraction studies at the APS include a pair of cryogen-free 4T magnets and one cryogenic 13T vertical field (belonging to MIT) located on the XOR 4-ID-D beamline. Various classes of problems that have been discussed in this conference can be studied using this set of three magnets using x-ray scattering techniques. A cryogenic 7T horizontal-field magnet that can be rotated to apply the field parallel and

perpendicular to the incident beam direction is operational on the 11-ID-C beamline. This magnet utilizes very high-energy (100 keV) x-rays to study crystallographic transitions in single crystals and powders.

A 13 T cryogenic vertical field magnet, similar to the one at the APS, is operational on a BM beamline at NSLS. Recent studies include competing order in La-Ba cuprates.

Finally, we note that there is an Oxford 15T vertical field magnet operational on the BL19LXU beamline at the Spring8.

6.3.2 Future directions

At the X-ray Magnet Facility session conceptual design of a future x-ray beamline and magnet capabilities were discussed. From the scientific presentations it was clear that there is a need to study materials primarily in small and high-quality single-crystal form using resonant and non-resonant diffraction and high-energy diffuse scattering techniques. Two such experiments that epitomized the requirements of the magnet and the versatility of an x-ray beamline were presented. Given the nature of measurements that must be carried out it was obvious that the magnet needs to have a large optical access and the sample needs to be tilted to access off-scattering plane points in reciprocal space. Secondly, a beamline that is flexible enough to easily accommodate energy tunability over a large range and polarization switching was envisioned. Finally, a goniometer with tilt and rotation mounted on top of the magnet for carrying out scans was discussed.

6.4 Neutron Instrument discussion

6.4.1 Neutron Instrument requirements

Types of measurements	Molecular magnets	Quantum magnetism	Systems with conduction electrons	Thin Films	Material Processing	Magnetic Resonance	Flux latices
Inelastic							
Q range	0-0.01Å $^{-1}$	0-5Å $^{-1}$	0-5Å $^{-1}$			0-3 Å $^{-1}$	
Q resolution	0.001Å $^{-1}$	0.02Å $^{-1}$	0.001Å $^{-1}$			10%	
E range	0-5meV,	0-50 meV	0-100meV			0-10meV	
E resolution	0.1meV	0.1meV or 5% of energy transfer	0.25meV or 5% of energy transfer			0.05meV	
Atomic scale diffraction							
Q range	0-0.01Å $^{-1}$	0-5Å $^{-1}$	0-5Å $^{-1}$		0-15Å $^{-1}$		0-0.01Å $^{-1}$
Q reolution	0.001Å $^{-1}$	0.02Å $^{-1}$	0.001Å $^{-1}$		0.02Å $^{-1}$		0.001Å $^{-1}$
SANS?	For crystallized molecular magnets	No	yes		Yes		yes
Reflectometry?	no	No	yes	yes		no	no
Types of samples							
Single crystal	possibly	Yes	yes			yes	yes
Powder?	powder	Yes with lower priority	yes		Yes	liquids	no
Thin films?	No	No	yes	yes			
Proton polarization for biological samples?	No	No	No	no		yes	no

Table 2 Neutron instrument requirements for a high magnetic field beam line at the SNS.

6.4.2 Preliminary analysis of a high magnetic field beamline at the SNS

The SNS facility offers several unique beamlines with differently optimized moderators that are potentially suitable for construction of a high field (40 T) magnet and the associated neutron scattering instrumentation. Specifically a cold-coupled moderator is available on beamline 14A and several locations on the decoupled water moderator are available. As seen in Table 2, the energy spectrum of the coupled cold moderator is

better matched to the majority of science discussed at the workshop. However either moderator would provide sufficient flux to enable world-class science. The two potential locations for the instrument are shown in Figure 35.

Figure 35 Potential high field magnet beamline locations on a site plan of the SNS

The science case drives the need for the highest fields. In collaboration with the National High Magnetic Field Laboratory in Tallahassee, it has been determined that a magnet of 35 – 40 T can be designed for scattering applications. Preliminary designs that were described in section 6.2 suggest two possible magnet configurations, and Figure 36 shows how both of these magnets can be accommodated on a single beamline:

1. A conical configuration with a 20° cone angle on the up and down stream side of the solenoid (labeled conical in Figure 36.)
2. A split magnet with 4, 45° degree openings equally spaced around the vertical cylinder with 5.7^o vertical acceptance and a 5mm gap. (labeled split in Figure 36)
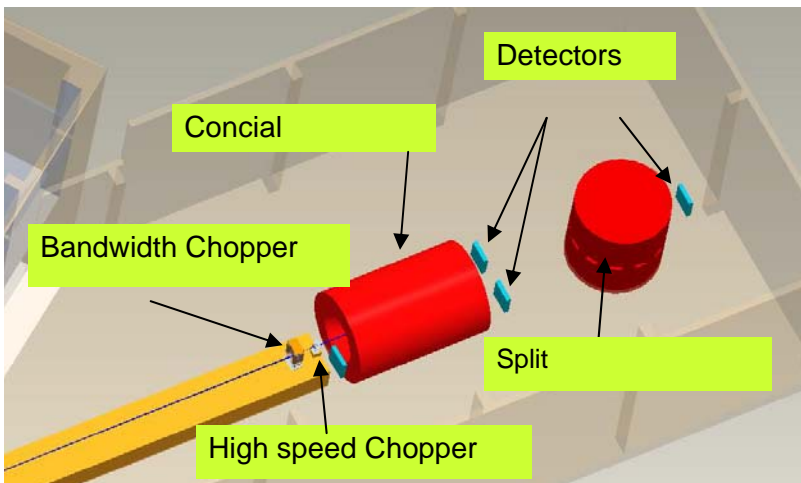

Figure 36 Region near the magnets for a high field magnet beamline at the SNS

With these magnets in mind, the remaining components of the neutron beamline can be specified to provide capabilities for a broad class of instrumentation. Specifically Atomic scale diffraction, large structure diffraction, reflectometry, and spectroscopy will be

accommodated. An analysis of the performance of an instrument with the parameters below has been performed.

- moderator: Shallow poison water moderator or cold coupled hydrogen
- Incident beam line: 80 m (70 m ± 10 m) of Ballisitic guide[114]
- Conical Magnet configuration:
  - o Field orientation: horizontal, parallel to beam
  - o Angular coverage 40° cone front and back
  - o Rotatable to provide two angular choices
    - -5° – 35° and -175° – -145°
    - -20° – 20° and 160° – 200°
  - o Sample
    - Size 20 mm x 20mm
  - o Specialized sample environment; flow cryostats with cryogen lines incident on upstream or penetration through top of magnet (reduction in field)
  - o Detectors: 1.5m long ^{3}He tubes ~ 4m from sample
    - 300, 10 mm diameter in forward scattering banks;
    - 57 25.4mm diameter in back scattering bank
- Split configuration
  - o Field orientation: vertical, perpendicular to beam
  - o Angular coverage ±5.7^o out of plane;15° spaced at 30° increments in plane
  - o Sample
    - Size 5 mm x 5mm
  - o Standard sample environment equipment
- Detectors: 1m long ^{3}He tubes ~ 4m from sample
  - o 300 10mm diameter tubes; 335 25.4mm diameter tubes
- 3 Bandwidth choppers
- High speed chopper (not in beamline for diffraction)
- Incident beam Polarization capabilities

For all the wide bandwidth instrumental configurations, this concept would provide a bandwidth of 0.8 Å. For atomic scale diffraction this bandwidth provides a useful flux of $3x10^6$ – 3 $x10^7$ n/s with a Q resolution of 1% over a Q range well suited to the science case for both single crystal and powder samples. For large scale diffraction this bandwidth provides a useful flux of $2x10^5$ – $7x10^6$n/s for the water moderator and gain of roughly 10x if the coupled cold moderator is utilized. A Q of 0.1Å^{-1} is the minimum attainable for this instrument. For Reflectometery a similar range of fluxes to the large scale diffraction will be provided and a minimum reflectivity of ~10^{-6} can be achieved.

For spectroscopy a high speed chopper will be introduced into the beam. When the chopper is spun to provide 5% resolution a flux of $5x10^5$ - $1x10^6$ n/s will be obtained at incident energies between 10-100 meV. If the chopper is slowed to provide 10% resolution the fluxes increase to $1x10^6$ – $3x10^6$ over the same energy range. As for the wide bandwidth cases, an additional order of magnitude in flux can be gained for incident

energies less than 20 meV if the instrument is placed on the cold coupled moderator. For systems where the energy transfer loss is less than ~ 75% of the incident energy, repetition rate multiplication[115] can be used for an additional gain of 3 - 6. Alternatively a set of Si crystals that would enable the instrument to work in a back scattering mode would enhance the performance of ultra high resolution studies like the neutron detected NMR described in section 0

In summary, a world class high magnetic field instrument can be built at the SNS. This instrument will excel in science that requires atomic scale diffraction, large scale diffraction, reflectometry, spectroscopy, or some combination. To ensure the optimal performance of this instrument, the magnets and the neutronic components of the instrument will be designed in concert.

7 Summary

The Probing Matter at High Magnetic Fields with X-Rays and Neutrons workshop detailed an exciting science case for the use of neutrons at High magnetic fields. For atomic scale systems a science case that encompassed: quantum magnets, magnetic molecules, High T_c superconductors, Collosal magneto resistance materials, Heavy Fermions, Metamagnets and the general measurement of spin Hamiltonians was detailed. For magnetic thin films, exchange biased systems, films of novel oxides, and highly anisotropic films were detailed. An extension of using scattering probes to study the structure of materials that are processed in a magnetic field for enhanced strength was presented. Several novel ideas were presented as well one of the most novel was to use neutrons to as the probe for nuclear magnetic resonance signals. The science requirements for a neutron instrument were derived from the science case and a preliminary concept for an instrument was presented.

8   Participants list

First	Last	Organization
Ian	Anderson	Oak Ridge National Laboratory
Mark	Bird	NHMFL
Greg	Boebinger	NHMFL
Paul C.	Canfield	Iowa State University
Roy K.	Crawford	Oak Ridge National Laboratory
Pengcheng	Dai	University of Tennessee
Carsten	Detlefs	ESRF
Allen	Ekkebus	Spallation Neutron Source/ORNL
Mechthild	Enderle	Institut Laue-Langevin
Mike	Fee	HTS-110
Michael	Fitzsimmons	Los Alamos National Laboratory
Paul	Follansbee	Los Alamos National Laboratory
Helmut	Fritzsche	National Research Council Canada
Flavio	Garcia	Brazilian Synchrotron Light Laboratory
J. Murray	Gibson	Argonne National Laboratory
Efim	Gluskin	Argonne National Laboratory
Garrett	Granroth	Spallation Neutron Source
Zahirul	Islam	Argonne National Laboratory
Shane Joseph	Kennedy	Australian Nuclear Science & Technology Organization
Helen	Kerch	US Dept of Energy
Tsuyoshi	Kimura	Los Alamos National Laboratory
Valery	Kiryukhin	Rutgers University
Alex	Lacerda	NHMFL-LANL
Bella	Lake	Iowa State University
Jonathan	Lang	Argonne National Laboratory
Seung-Hun	Lee	University of Virginia
Wai Tung	Lee	Oak Ridge National Laboratory
Young	Lee	Massachusetts Institute of Technology
Gabrielle	Long	Argonne National Laboratory
Gerry	Ludtka	Oak Ridge National Laboratory
Mark	Lumsden	Oak Ridge National Laboratory
Pascal	Manuel	ISIS Facility
Brian	Maple	University of California at San Diego
Thom	Mason	SNS
Ferenc	Mezei	HMI
John	Miller	NHMFL
Christie	Nelson	Brookhaven National Laboratory
Tom	Painter	NHMFL
Karel	Prokes	Hahn-Meitner-Institute
Christine	Rehm	American Scientific Instrumentation
Yang	Ren	Argonne National Laboratory
James	Rhyne	Los Alamos National Laboratory
George	Srajer	Advanced Photon Source
Jorg	Strempfer	Max-Planck Institute for Solid State Research

Raymond	Teller	Argonne National Laboratory
Guebre	Tessema	NSF
Christian	Vettier	Institut Laue-Langevin (ILL)
Igor	Zaliznyak	Brookhaven National Laboratory

9 References

[1] C. Broholm *et al.,* p. 77-105 in "Dynamical Properties of Unconventional Magnetic Systems" edited by A. T. Skjeltorp and D. Sherrington, NATO ASI Series, Series E: Applied Sciences vol. 349, Kluwer Academic Publishers, Boston (1998).

[2] A. Müller, C. Serain Acc. Chem. Res. **33**, 2 (2001); P. Kögerler, A. Müller Polyoxometalate Science Kluwer Academic Publishers pp297-323 (2003).

[3] J. Schnack, M. Luban, and R. Modler, *Europhys. Lett*. **56**, 863 (2001).

[4] V. O. Garlea *et al.*, submitted to *Phys. Rev. Lett*. (cond-mat/0505066)

[5] T. Giamarchi, Quantum Physics in One Dimension, Oxford University Press (2004).

[6] M. Kenzelmann *et al.*, Phys. Rev. Lett. **93**, 017204 (2004).

[7] M. B. Stone *et al.*, Phys. Rev. Lett. **91**, 037205 (2003).

[8] D. C. Dender *et al.*, Phys. Rev. Lett. **79**, 1750 (1997).

[9] I. Affleck and M. Oshikawa, Phys. Rev. B **60**, 1038 (1999).

[10] F. D. M. Haldane, Phys. Rev. Lett. **50**, 1153 (1983).

[11] I. Affleck *et al.*, Phys. Rev. Lett. **59**, 799 (1987).

[12] S. Ma *et al.*, Phys. Rev. Lett., 69, 3571 (1992).

[13] I. A. Zaliznyak, S.-H. Lee, and S. V. Petrov, Phys. Rev. Lett. **87**, 017202 (2001).

[14] A. Zheludev *et al.*, Phys. Rev. B **69**, 054414 (2004).

[15] Y. Chen *et al.* , Phys. Rev. Lett. **86**, 1618 (2001).

[16] M. Kenzelmann *et al.*, Phys. Rev. Lett. **90**, 087202 (2003).

[17] T. Waki *et al.*, J. Phys. Soc. Japan **73**, 3435 (2004).

[18] B. S. Shastry and B. Sutherland, Phys. Rev. Lett. **47**, 964 (1981).

[19] I. Affleck, Phys. Rev. B **43**, 3215-3222 (1991).

[20] G. Xu *et al.*, Phys. Rev. Lett. **84**, 4465 (2000).

[21] M. Hase *et al*., Phys. Rev. Lett. **70**, 3651 (1993).

[22] M. Shaz *et al.*, Phys. Rev. B **71**, 100405(R) (2005).

[23] T. Sasaki *et al.*, cond-mat/0501691

[24] C. Broholm *et al.*, p 211-234 in "High Magnetic Fields – applications in condensed matter physics and spectroscopy" C. Berthier, L. P. Lévy, and G. Martinez, Eds. Springer Verlag (2002).

[25] Matthew B. Stone *et al.*, submitted to Nature (2005).

[26] K. P. Schmidt, C. Knetter, and G. S. Uhrig, Phys. Rev. B **69**, 104417 (2004).

[27] M. Azuma *et al.*, Phys. Rev. B **62**, R3588 (2000).

[28] Y. Qiu *et al.*, Phys. Rev. B **71**, 214439 (2005).

[29] A. Süto, Helv. Phys. Acta **54**, 191 (1981); 201 (1981).

[30] P. Sindzingre *et al.*, Phys. Rev. Lett. **84**, 2953-2956 (2000).

[31] M. E. Zhitomirsky, Phys. Rev. Lett. **88**, 057204 (2002).

[32] A. P. Ramirez, B. Hessen, and M. Winklemann, Phys. Rev. Lett. **84**, 2957-2960 (2000).

[33] B. S. Shastry and B. Sutherland, Physica (Amsterdam) **108B**, 1069 (1981).

[34] B. D. Gaulin *et al.*, Phys. Rev. Lett. **93**, 267202 (2004).

[35] H. Kageyama *et al.*, Phys. Rev. Lett. **82**, 3168 (1999).

[36] M. Oshikawa, M. Yamanaka and I. Affleck, Phys. Rev. Lett. **78**, 1984 (1997).

[37] M. Oshikawa, Phys. Rev. Lett. **84**, 1535 (2000).

[38] W. Shiramura *et al.*, J. Phys. Soc. Jpn. **67** 1548 (1998).

[39] B. C. Watson *et al.*, Phys. Rev. Lett. **86**, 5168 (2001).

[40] T. Ono *et al*., Phys. Rev. B **67**, 104431 (2003).

[41] M. Uchida and H. Tanaka, Phys. Rev. B **66**, 054429 (2002)

[42] Y. Narumi *et al.,* Physica B **246,** 509 (1998).

[43] Ch. Ruegg *et al*., Phys. Rev. Lett. **93**, 037207 (2004).

[44] Y. Hosokoshi, Y. Nakazawa and K. Inoue, Phys. Rev. B **60**, 12924 (1999).

[45] R. Moessner and J. T. Chalker, Phys. Rev. Lett. **80**, 2929-2932 (1998).

[46] S.-H. Lee *et al.*, Nature **418**, 856 (2002).

[47] H. Ueda *et al.*, Phys. Rev. Lett. **94**, 047202 (2005).

[48] J. S. Gardner *et al*., Phys. Rev. Lett. **82**, 1012 (1999).

[49] I. Mirebeau *et al.*, J. Phys. Cond. Matt. **17**, 8771 (2005).

[50] S. Mitsuda *et al.*, J. Phys. Chem. Solids **60**, 1249 (1999).

[51] S. Mitsuda *et al.*, J. Phys. Soc. Jpn. **69**, 33 (2000).

[52] A. P. Ramirez, Ann. Rev. Mat. Sci. **24**, 453 (1994).

[53] H. Katsura, N. Nagaosa, and A. V. Balatsky, Phys. Rev. Lett. **95** (2005).

[54] T. Kimura *et al.*, Nature **426**, 55 (2003).

[55] L. C. Chapon *et al.*, Phys. Rev. Lett. **93** (2004).

[56] R. Coldea *et al.*, Phys. Rev. Lett. **88**, 137203 (2002).

[57] M. B. Stone *et al.*, Phys. Rev. B **64**, 144405 (2001).

[58] B. Lake *et al.*, *Science* **291** (2001) 1759.

[59] J. M. Tranquada *et al.*, Phys. Rev. B **69**, 174507 (2004).

[60] B. Lake *et al.*, *Nature* **415** (2002) 299.

[61] B. Khaykovich *et al.*, Phy. Rev. B **67**, 054501 (2003).

[62] Pengcheng Dai *et al.*, *Nature* **406** 965 (2000).

[63] M. Tokunaga, *et al.*, Phys. Rev. B, **57**, 5259 (1998).

[64] J. A. Fernandez-Baca, *et al.*, Phys. Rev. B, **66**, 054434 (2002).

[65] T. Kimura, *et al.*, Nature **426**, 55 (2003).

[66] T. Goto, *et al.,* Phys. Rev. Lett. **92**, 257201 (2004).

[67] K. Fujita, T. Mochida, and K. Nakamura, Jpn. J. Appl. Phys. **40** (2001) 4644.

[68] T. Motohashi, *et al.*, Phys. Rev. B **67**, 064406 (2003).

[69] Y. Wang *et al.*, Nature **423**, 425 (2003).

[70] Takada *et al.,* Nature **422**, 53 (2003).

[71] K. Fujita, T. Mochida, and K. Nakamura, Jpn. J. Appl. Phys. **40** (2001) 4644.

[72] R. Jin, B.C. Sales,P. Khalifah, and D.Mandrus, cond-mat/0306066 (2003).

[73] F.C. Chou, *et al.*, cond-mat/0306659 (2003).

[74] L. Balicas, *et.al.*, cond-mat/0410400 (2004).

[75] K. H. Kim *et al.*, Phys. Rev. Lett **91,** 256401 (2003).

[76] T.E. Mason *et al.* , J. Phys.: Condens. Matter **7**, 5089 (1995).

[77] J.A. Paixão, *et al.*, Phys. Rev. Lett. **89**, 187202 (2002).

[78] W.H. Meiklejohn and C.P. Bean, Phys. Rev. B **102** 1413 (1956).

[79] J. Nogués, Ivan K. Schuller, J. Magn. Magn. Mater. **192** 203 (1999).

[80] Y. Ijiri, *et al.*, Phys. Rev. Lett. **80** 608 (1998).

[81] E.E. Fullerton, S.D. Bader, J.L. Robertson, Phys. Rev. Lett. **77** 1382 (1996).

[82] A. Schreyer *et al.,* J. Appl. Phys. **87** 5443 (2000).

[83] M. Fitzsimmons, D. Belanger, D. Lederman, unpublished.

[84] J. Nogués,*et al.*, Phys. Rev. B **61** R6455 (2000).

[85] J. Nogués, C. Leighton, Ivan K. Schuller, Phys. Rev. B **61** 1315 (2000).

[86] S. de Brion, *et al.*, Eur. Phys. J. B **33** 413 (2003).

[87] W. Prellier,*et al.*, Phys. Rev. B **66** 024432 (2002).

[88] M. J. Bentall, *et al.*, J. Phys.: Condens. Matter **15**, 4301 (2003); H. Fritzsche *et al.*, unpublished

[89] G. M. Ludtka *et al.*, *Scripta Materialia* **51** (2004) 171–174.

[90] D. M. Nicholson *et al.*, *Journal of Applied Physics* **95**, No. 11 (June 2004) 6580–6582.

[91] R. A. Jaramillo *et al.*, *Scripta Materialia* **52** (2005) 461–466 .

[92] G. M. Ludtka *et al*, U.S. DOE Industrial Materials for the Future Project Final Report, ORNL/TM-2005/79, March 2005.

[93] G. M. Ludtka *et al.*, *Proceedings of the International Workshop on Materials Analysis & Processing in Magnetic Fields*, ed. H. J. Schneider-Muntau and H. Wada, National High Magnetic Field Laboratory of Florida State University, Tallahassee Florida, March 16–19, 2004, in press.

[94] G. M. Ludtka et al., *Metallurgical and Materials Transactions A*, in preparation.

[95] R. A. Jaramillo *et al.*, *Proceedings of the TMS Conference on Solid-Solid Phase Transformations in Inorganic Materials 2005,* to be held May 29–June 3, 2005, Phoenix, AZ, in preparation.

[96] M. R. Eskildsen *et al.*, Phys. Rev. Lett. **78**, 1968 (1997).

[97] D. McK. Paul *et al.*, Phys. Rev. Lett. **80**, 1517 (1998).

[98] R. Gilardi, *et al.*, Phys. Rev. Lett. **88**, 217003 (2002).

[99] M. R. Eskildsen, *et al.*, Phys. Rev. Lett. **90**, 187001 (2003).

[100] S. P. Brown, *et al.*, Phys. Rev. Lett. **92**, 067004 (2004).

[101] R. Gilardi, *et al.*, Phys. Rev. Lett. **93**, 217001 (2004).

[102] M. Yethiraj, *et al.*, Phys. Rev. B **72**, 060504(R), (2005).

[103] V. G. Kogan, *et al.*, Phys. Rev. B **55**, R8693 (1997).

[104] V. G. Kogan, *et al.*, Phys. Rev. Lett. **79**, 741 (1997).

[105] N. Nakai, *et al.* , Phys. Rev. Lett. **89**, 237004 (2002).

[106] R. Cubitt, *et al.*, Phys. Rev. Lett. **91**, 047002 (2003).

[107] D. Pal, *et al.*, submitted to Physical Review B (rapid communication).

[108] "The Hydrogen Initiative", Report of the Energy Subcommittee of the American Physical Society Panel On Public Affairs, APS, March 2004, Brian Clark, Daniel Cox, Craig Davis, Peter Eisenberger, Bill Evenson, Barbara Levi, Francis Slakey, Jennifer Zinck, Linda Capuano, Linda Cohen, Mildred Dresselhaus and Susan Fuhs.
http://www.aps.org/public_affairs/loader.cfm?url=/commonspot/security/getfile.cfm&PageID=49633

[109] S. K. Misra *et al.*, J. Magn. Reson. **174**, 265 (2005).

[110] P. P. Borbat *et al.*, *Science* **291**, 266 (2001).

[111] E.J. Hustedt, and A.H. Beth,. *Biophys. J.* **86**, 3940 (2004).

[112] J. R. Miller, and M. D. Bird, "A New Series-Connected Hybrid Magnet System for the National High Magnetic Field Laboratory", *IEEE Trans. On Appl. Supercond*. Vol. 14, no. 2, pp 1283-1286.

[113] M. D. Bird, S. Bole, S. Gundlach, and J. Toth, "Conceptual Design of Split and Conical Powered Magnets at the NHMFL", presented 19th International Conference on Magnet Technology, Genoa, Italy, Sept. 19 – 23, 2005

[114] F. Mezei, M. Russina, and M. Schorr, Physica B **276-278**, 128 (2000); C. Shanzer *et al.*, Nucl. Inst. and Meth. A **529**, 63 (2004).

[115] F. Mezei, J. Neutron Res., **6**, 3 (1997).